IOP Publishing

Smart Surface Design for Efficient Ice Protection and Control

Carlo Antonini and Irene Tagliaro

Chapter 2

Strategies for icephobicity and the role of surface chemistry

Simrandeep Bahal, Miisa Tavaststjerna, Navid Mostofi Sarkari, Anny Catalina Ospina Patino, Gabriel Hernandez Rodriguez, Alexandros A Atzemoglou, Theodoros Dimitriadis, David Seveno, Irene Tagliaro, Manish K Tiwari and Vikramjeet Singh

2.1 Introduction

Ice accretion on surfaces is one of the fundamental problems presented by nature, and the effects of ice accumulation can be observed on aircraft surfaces, the blades of wind turbines, electrical cables, refrigeration systems, and in many other places [1]. Broadly, this phenomenon of icing has some serious detrimental effects in the aviation and power sectors and on infrastructure such as buildings and bridges [2]. For example, ice build-up on an aircraft's wing disrupts the normal flow of the air over the wing and hence leads to a loss of lift force, which can result in the stalling of the aircraft even at higher speeds [1]. In the case of wind turbine blades, the presence of ice causes a weight disparity and reduces the aerodynamic performance, resulting in lower power generation [2]. In heating, ventilating and air conditioning (HVAC) applications, the formation of ice around the compressor lowers the efficiency of the system and can also clog the system's fans [1]. In household applications, such as in dish antennas, the ice build-up interferes with the electromagnetic signal detection and leads to poor quality signal at the end user output devices. Considering all these detrimental effects of icing in various applications, it would be quite useful to prevent the formation of ice or remove the ice from the various substrates as soon as it builds up. There are various methods of ice removal from a surface, and these methods have been classified into two categories, namely active and passive [3]. Active systems require energy from a source and consist of mechanical, thermal, chemical and electrical methods [1]. On the other hand, passive systems comprise specialized materials or the application of various coatings on the substrate to render icephobic/anti-icing properties to the substrate. Therefore, it is important to understand the theory behind ice nucleation on the substrates to design surfaces that

doi:10.1088/978-0-7503-6009-8ch2

thermodynamically inhibit the formation of ice. The following two sections discuss the mechanism of ice nucleation on a surface and the different types of ice nucleation.

2.1.1 Ice nucleation theory

The phase change of water plays an important role in many natural phenomena such as cloud and fog formation and the precipitation of rain and snow. In industrial and technical applications such as in heat exchangers, condensers and water desalination applications, a high nucleation and condensation rate of water is desired. On the other hand, in the design of anti-icing substrates, the suppression of water and ice nucleation is sought. A phase change occurs when the original or the mother phase has turned into a supersaturated phase. The development of a new phase from the original supersaturated mother phase does not occur in a continuous manner, but it occurs in a spontaneous manner due to fluctuations in density and temperature. This spontaneous process is termed nucleation. Many nucleation theories have been proposed to describe the kinetics of nucleation, but the classical nucleation theory has been the most widely used theory to study the effects of nucleation [4]. This theory is based on two major assumptions. First, the nuclei or the embryos are spherical clusters with macroscopic density and surface tension. Second, the clusters are distributed according to the Boltzmann statistical theory [5].

Nucleation can be further divided into two types—homogeneous and heterogeneous. When the nucleation takes place within the liquid phase itself away from any foreign surfaces, it is termed as homogeneous nucleation. On the other hand, when the nucleation occurs on an external solid substrate, it is known as heterogeneous nucleation.

2.1.1.1 Homogeneous nucleation

In the case of homogeneous nucleation, a growing ice embryo of clustered water molecules is modeled as a sphere of radius r_e. When the temperature of the liquid is reduced below the freezing temperature at a given pressure, the liquid becomes supercooled and is said to be in a metastable state. In liquid water, a cluster of a few molecules due to random agglomeration of molecules is always present [6]. There is a continuous formation and decay of these agglomerates. When the liquid water is in a supercooled, metastable state, the formation of such a cluster is energetically favored due to the difference in the chemical potential. The chemical potential of a molecule within the cluster is reduced compared to the liquid phase. However, the formation of a cluster is also energetically costly because it also leads to the formation of a new interface, namely the ice–liquid interface. Hence, the total change in the free energy of the liquid water due to the formation of a spherical ice embryo is the sum of two competing energy effects. First is the formation of a new lower-energy solid (ice) phase. The second is the creation of a new high-energy ice–liquid interface. The expression for the same is represented as [6]

$$\Delta G\ (T, r_e) = -\frac{4}{3}\pi r_e^3 \Delta G_{IW}(T) + 4\pi r_e^2 \gamma_{IW}(T). \tag{2.1}$$

In the above expression, $\Delta G_{IW}(T)$ denotes the free energy difference between ice and water per unit volume and $\gamma_{IW}(T)$ represents the interfacial energy (per unit area) of the ice–water interface. The first term in the above equation represents the decrease in the free energy of the volume which is occupied by the ice embryo during the phase change from liquid to solid. On the other hand, the second term represents the increase in the surface energy due to the newly formed ice–liquid interface. At low radii, the interfacial energy term dominates whereas at higher embryo radii, the volume energy term dominates. The curve of the Gibbs free energy ΔG with the embryo radius r_e is shown in figure 2.1.

By differentiating the free energy term, ΔG in the equation (2.1) with respect to the ice embryo radius r_e, and setting the resulting equation equal to zero, we can find the critical embryo radius r_e^*. If the radius of the ice embryo is less than the critical radius, then it is energetically favorable for the ice embryo to decay back into the liquid phase. On the other hand, if the ice embryo has grown to a critical radius, then it is energetically favorable for the embryo to keep on growing into the solid ice phase. The expression for the critical embryo radius comes as

$$r_e^* = \frac{2\gamma_{IW}}{\Delta G_{IW}}. \tag{2.2}$$

The critical embryo radius depends upon the free energy of the ice–water interface γ_{IW} and the free energy difference between ice and water per unit volume ΔG_{IW}. To calculate ΔG_{IW}, Gibbs–Helmholtz equation can be used.

At the critical embryo radius r_e^*, the free energy barrier ΔG^* can be found by plugging equation (2.2) into equation (2.1):

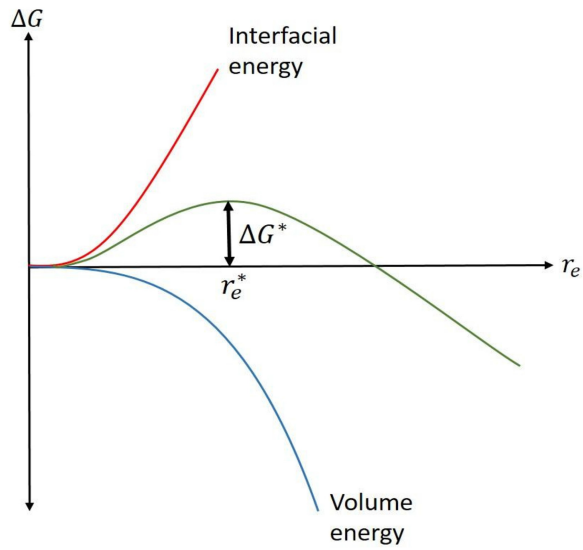

Figure 2.1. Effect of the radius of the ice embryo r_e on the Gibbs free energy ΔG. ΔG^* is the free energy barrier for continuous ice growth and r_e^* is the critical embryo radius.

$$\Delta G^*(T) = \frac{16\pi\gamma_{IW}(T)^3}{3(\Delta G_{IW}(T))^2}. \tag{2.3}$$

2.1.1.2 Heterogeneous nucleation

In day-to-day life, nucleation of ice embryo is more likely to occur at the liquid–solid interface than within the supercooled liquid itself [7]. Hence, it is important to determine the free energy barrier for the case of heterogeneous nucleation to to design and develop surfaces with anti-icing characterstics [8]. The classical nucleation theory was adapted for the case of heterogeneous nucleation by Fletcher [9]. Fletcher considered a spherical ice embryo of radius r_e growing on a convex substrate with roughness radius R_s within a liquid phase. The free energy of formation of ice embryo for this case can be written as [6]

$$\Delta G(T, r_e, R_s) = \Delta G_{IW} V_I + \gamma_{IW} SA_{IW} + (\gamma_{IS} - \gamma_{SW}) SA_{IS}. \tag{2.4}$$

In the above equation, ΔG_{IW} is the free energy difference between ice and water per unit volume, V_I is the volume of the ice embryo, SA_{IW} is the interfacial area between the ice embryo and the water, and SA_{IS} is the interfacial area between the ice embryo and the substrate. γ_{IS} and γ_{SW} represent the interfacial energies (per unit area) between the ice embryo and solid substrate, and solid substrate and water, respectively. Fletcher noted that a foreign solid substrate creates a low energy interface between the ice embryo and the solid substrate. Hence the third term in the above equation (2.4) would be negative. Hence the magnitude of the Gibbs free energy for heterogeneous nucleation is less than that of homogeneous nucleation. After doing some geometric manipulations, the free energy barrier for the heterogeneous growth of a stable ice embryo is given as

$$\Delta G^*(T) = \frac{16\pi\gamma_{IW}(T)^3}{3(\Delta G_{IW}(T))^2} f\left(\theta_{IW}, R_s\right), \tag{2.5}$$

where f is the geometric factor and depends upon the ice–water contact angle θ_{IW} and the radius of curvature of the surface roughness R_s. It can be seen that equations (2.5) and (2.3) are nearly identical with the only difference being the presence of an additional wetting factor f in equation (2.5). The value of f is always less than 1. Hence $\Delta G^*_{heterogeneous} < \Delta G^*_{homogeneous}$. This implies that ice nucleates with more ease on a foreign solid substrate.

2.1.2 Characteristics of icephobic surfaces

Icephobic surfaces have three main properties. They should be able to repel incoming liquid water droplets, delay the freezing of water droplets and lower the adhesion strength between the ice and the underlying substrate [10].

2.1.2.1 Repelling incoming water droplets

The first property of an icephobic surface is to repel incoming water droplets. In this way, the surface will be free of any liquid water before freezing occurs. For this, it is

desired that the surface should be able to repel the incoming water quickly with a short contact time and without losing its water-repellent performance. A super-hydrophobic surface was designed with micrometer-sized pillars decorated with a nanometer-sized texture to study the drop impact using supercooled water droplets [3]. The authors found that supercooled droplets even at −30 °C could be repelled by their designed surface.

2.1.2.2 Delaying the freezing of water droplets

In the situations where a sufficiently fast removal of liquid droplets is not possible, there is another option to achieve the icephobic property which is to delay the freezing of water droplets as long as possible. The freezing delay can be measured in terms of ice nucleation temperature [11] and the freezing delay time. The ice nucleation temperature is defined as a temperature at which a sessile water droplet placed on a surface nucleates into ice when the droplet is cooled in a slow and quasi-equilibrium manner. The freezing delay time is the average time taken by a supercooled droplet placed on a surface to nucleate into ice [12].

2.1.2.3 Reducing the ice adhesion strength

In the cases where freezing is inevitable, it is favorable to reduce the adhesion strength between the ice and the underlying substrate so that the ice can be removed easily by external forces such as by the aid of gravity or wind shear. Typically, it is considered that a surface has a low adhesion to ice when the adhesion strength is below 100 kPa and super low ice adhesion when the adhesion strength is below 10 kPa [13].

2.2 Wettability and its relation to icephobic properties

2.2.1 Liquid–solid interaction

The interaction of ice with a surface understandably elicits parallels with liquid–solid interactions and, often, the two sets of interactions are related. However, the relation is not straightforward. Therefore, a quick review of the surface wettability and liquid–solid interaction is in order. The wettability of a surface can be described based on its behavior toward a fluid or as the balance between the surface and interfacial forces. The outcome of an impacting droplet can be characterized either as wetting or anti-wetting and is dependent on the properties of the substrate. This property is of substantial significance when defining the surface chemistry, physics and engineering applications of a material.

The determination of wettability is based on the measurement of the surface contact angle. Contact angle is the main parameter that characterizes the shape of a droplet on a solid surface. The wettability depends on the surface roughness and chemical composition [14]. Changes to these parameters can adjust the value of the contact angle and hence affect the wettability (figure 2.2).

2.2.1.1 Mechanism and definitions of non-wettability

To characterize a surface as non-wettable, it is essential that any drop can be removed with ease, by applying only a small force (a fraction of the drop weight).

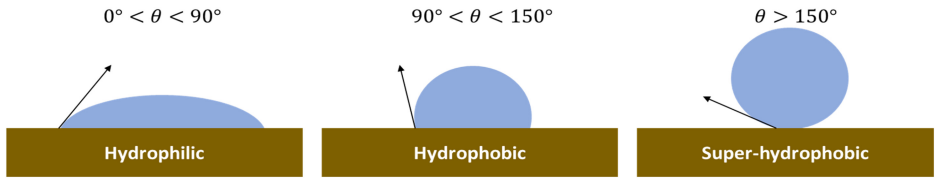

Figure 2.2. Conventional definition of surface wettability: hydrophilic having a contact angle with water smaller than 90°, hydrophobic with an angle greater than 90°, and superhydrophobic with contact angle greater than 150°.

This is typically assessed by tilting the surface, similar to the natural inclination of leaves, and measuring the contact angle at which the droplet rolls off. For a surface to be non-wettable, it is important that the contact angle of a droplet is greater than 150° and the roll-off angle is less than 5°. The easy removal of a drop from a solid surface appears to be dependent on two main factors: (i) the ability of a weak external force to move the drop out of equilibrium and (ii) a high rate of removal from the surface. These two factors characterizing non-wettability translate into the following objectives: (i) minimizing hysteresis by ensuring surface uniformity and (ii) maximizing the contact angle. In theory, both goals can be achieved if the surface interacting with the liquid predominantly consists of gas, such as air trapped within surface roughness grooves [15].

A qualitative definition could suggest that the wetted area has to be sufficiently small. Overall, it is evident that in order to be non-wettable the solid surface must be either rough or porous. The grooves of a rough surface are interconnected and open to the atmosphere. In a porous surface, the pores may be either interconnected or isolated. In the latter case it may be much easier to keep the air in the pores in a stable state, but structural constraints may limit the reduction of the wetted area.

A superhydrophobic surface can even be observed with the bare eye. When a flow of water is applied on the substrate surface, an intuitional wetting behavior and a self-cleaning phenomenon are observed. However, determination of the static water contact angle (WCA) and contact angle hysteresis (CAH), are essential to quantitatively characterize the superhydrophobic property. It is well known that superhydrophobic surfaces can exhibit completely different contact angle hysteresis. Five different wetting states have been described, to differentiate the different superhydrophobic states: totally wetting superhydrophobic surfaces in the Wenzel state, totally air-supporting superhydrophobic surfaces in the Cassie state, the metastable state between the Wenzel and Cassie states (including a 'petal' state), surfaces in the micro/nanostructured two-tier 'lotus' state, and a partially wetting 'gecko' state [16].

2.2.1.2 Artificial super-liquid-repellent surfaces

Natural liquid-repellent surfaces have inspired scientists to develop a range of superhydrophobic and superoleophobic surfaces. Modifying the surface structure and chemical composition are the two key parameters for creating liquid-repellent surfaces. However, fabricating superoleophobic surfaces is significantly more

challenging than producing superhydrophobic ones [17]. Therefore, it is essential to control both the surface chemical composition and the surface geometry for the fabrication of superamphiphobic surfaces.

2.2.1.3 Surface structure

Designing the appropriate surface structure constitutes the first step for the fabrication of super-non-wetting surfaces. A suitable roughness can provide a capillary force that prevents liquid from entering into the grooves on the surface. Different methods have been employed for the fabrication of super-non-wettable surfaces, such as grinding, sandblasting, particle coatings, etching, and lithography, which have been used for surface roughening. After surface roughening, the air can be trapped inside the fabricated grooves. This trapped air provides a floating force against the liquid droplets, which is important to achieve a low sliding angle and low contact angle hysteresis.

2.2.1.4 Chemical modification and interfacial energy

Achieving the desired wettability greatly depends on the chemical composition of a material, which plays a crucial role in determining its surface free energy. For a liquid-repellent surface, the contact angle of a liquid droplet should be greater than 90°. Additionally, the surface free energy of the solid substrate should be less than one-quarter that of the liquid. Studies have shown that surface energy levels in monolayer films follow this order: $–CH_2 > –CH_3 > –CF_2 > –CF_2H > –CF_3$. Fluoropolymers, which contain high levels of $–CF_3$ and $–CF_2$ groups, are widely used to reduce surface energy. These materials also offer other benefits, including good chemical and thermal stability and a low friction coefficient [18].

2.2.1.5 Strategies for ice mitigation relying on liquid–solid interactions

The rational design of potential icephobic devices should fulfill requirements in three sequential categories (adapted from [2]) below. Theoretical and experimental evidence suggests that high receding contact angles are beneficial for effective de-icing. However, further development of the equations for ice shedding has revealed that crack size plays a more critical role in determining ice adhesion strength [26].

(i) *Repelling water before it holds on to the surface:* An initial approach to achieving low ice adhesion in materials is based on the idea that preventing surface interactions with liquid water may be crucial. The similar surface free energies of water and ice seem to support this strategy. However, it is important to note that, in the early stages of design, understanding the conditions under which water will approach the surface is essential. For instance, depending on the application, water may contact the surface as vapor, liquid, supercooled droplets, or, under colder conditions, as a solid. Numerous studies have sought to establish a relationship between wetting properties and ice adhesion behavior. While ice adhesion strength generally decreases with increasing hydrophobicity, experimental advances indicate that wettability alone is not a reliable predictor of icephobic behavior in all cases [19–21].

(ii) *Delaying freezing (nucleation) of sessile droplets:* The second requirement addresses the phase change from liquid water to solid ice once water is present on the surface. At this stage, hydrophobic and icephobic behaviors must be compared, highlighting their similarities and differences as explored in several studies. An interesting modeling study investigated the nucleation efficiency during this phase transition. Lupi *et al* designed carbon surfaces with both homogeneous and heterogeneous distributions of hydrophilicity [22]. Their findings suggest that, beyond the hydrophilic character itself, the spatial distribution of hydrophilic areas on the surface significantly influences heterogeneous ice nucleation efficiency by affecting the organization of water molecules at the interface. They observed that the nanoscopic layering in the interfacial region correlates more strongly with ice nucleation efficiency than wettability, according to theoretical molecular dynamics simulations. Consequently, intrinsic wettability, which plays a key role in phase change processes such as boiling and condensation, may not be as effective for controlling ice nucleation behavior. Additional studies have since been conducted to identify surface properties beyond wettability that are critical for understanding the speed of ice nucleation [23].

(iii) *Facilitating ice removal*: Once ice forms on the surface, a solid–solid interaction perspective is essential to understand the ice adhesion strength of the surfaces [24]. As explained by Nosonovsky *et al*, water can withstand compressive or tensile forces but cannot endure shear stress, whereas ice can sustain both shear loads and distributed normal stress [25].

As summarized in figure 2.3, designing icephobic surfaces involves more than simply addressing the adhesive interactions between liquid water and a solid surface. Although water maintains the same chemical composition across different states, its mechanical, thermodynamic, physicochemical, and surface properties differ significantly between liquid and solid phases, making direct extrapolation impossible. Therefore, understanding de-wetting and ice detachment from solid surfaces requires integrating models from liquid, solid, and transitional phases. Given the challenges of controlling all relevant conditions simultaneously, the most practical approach for achieving effective icephobic behavior is to design materials tailored to the specific environmental conditions of the intended application.

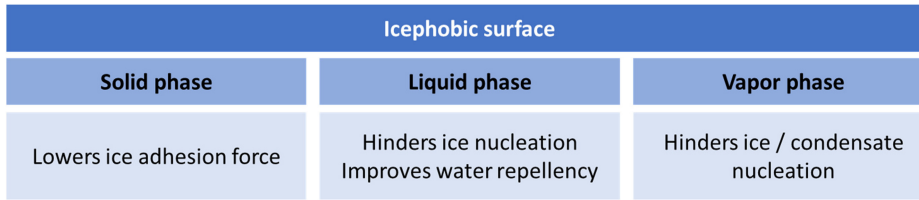

Figure 2.3. Interaction of icephobic surfaces with water in different condensed states.

2.2.1.5.1 Superhydrophobic anti-icing surfaces

Although terms such as 'superhydrophobic' and even 'hydrophobic' remain debated in the literature [27], superhydrophobicity is generally defined as surfaces that ensure water repellence (high contact angles) and high droplet mobility (low contact angle hysteresis) [28]. This effect is typically achieved with rough or hierarchical surfaces, which promote a Cassie–Baxter wetting state. The potential of these surfaces for icephobic design can be assessed based on the previously outlined stages.

Superhydrophobic properties are particularly useful in the initial stage of ice formation, as they can delay water retention by causing liquid or supercooled droplets to rebound or roll off the surface. The air pockets within these surfaces may also act as thermal barriers, reducing freezing rates and lowering ice nucleation efficiency [29, 30]. This makes superhydrophobic surfaces (SHSs) advantageous for developing passive anti-icing systems [26]. However, under high humidity, these textures can promote water droplet condensation, as will be discussed later. Compared with smooth hydrophobic surfaces, superhydrophobic surfaces have shown a significant delay in freezing, a beneficial characteristic in the second stage of ice formation.

A recent review suggests that to control freezing propagation (e.g. through ice bridging, cascade freezing, frost halos, or droplet explosions) [26], it is crucial to manage condensation by precisely designing surface structures. This includes spacing between pillars and optimizing both wettability and roughness to prevent or delay ice propagation under specific environmental conditions. In the final stage, once ice begins to form on the surface, superhydrophobicity can help achieve icephobicity by correlating high receding contact angles and low contact angle hysteresis with reduced ice adhesion strength [31].

Nonetheless, discrepancies persist between expected and actual ice adhesion strength measurements. Theoretical work has shown that microcrack size at the solid interface is a key factor in ice adhesion, indicating that in the third stage of ice testing, the surface should ideally provide sufficient voids at the interface. This characteristic, however, does not always align with the properties of highly superhydrophobic surfaces. As a result, while superhydrophobicity is promising for delaying freezing by enhancing water shedding, it does not always guarantee low ice adhesion. Experiments have shown that this anti-icing effect persists down to −20 °C, regardless of surface effusivity and wettability. Understanding the environmental conditions and wetting mode is crucial for selecting the appropriate approach and material.

2.2.1.6 Delay of icing on superhydrophobic surfaces

Superhydrophobic surfaces employ two main strategies to prevent and delay ice formation: reducing the contact time of water on the surface and hindering heterogeneous nucleation through surface design [32]. For the first approach, superhydrophobic coatings aim to shed most of the liquid water impacting the surface before ice can nucleate and spread. High water repellency of these surfaces is achieved through low surface energy, causing droplets to either rebound directly or be shed by external forces such as gravity, wind, vibrations, or larger droplet sizes

[33]. On superhydrophobic surfaces, water droplets tend to adopt a spherical shape, minimizing contact area with the solid and allowing droplets to roll off with minimal tilting angles [34].

Superhydrophobic surfaces are typically created by increasing surface roughness and/or chemically modifying the surface with low-energy compounds. The combination of roughness and chemical modification has been shown to enhance icephobic properties [35]. Studies have found that materials with low dielectric constants exhibit weak ice adhesion, as they do not contribute to electrostatic attraction with water molecules, making them ideal candidates for icephobic applications. Perfluorinated polymers, for example, are of particular interest due to their low dielectric properties. Poly(tetrafluoroethylene) (PTFE, commercially known as Teflon®) has a low electrical permittivity of about 2.1, making it a strong candidate for minimizing electrostatic interactions with water molecules. When PTFE coatings are applied to aluminum substrates, they form submicron grain structures with gaps smaller than the average water droplet size. These gaps trap air, allowing the surface to achieve a Cassie–Baxter state. The trapped air in these surface defects not only reduces the actual contact angle, thereby lowering ice adhesion, but also provides stress points that promote crack propagation during ice removal. Additionally, the air pockets serve as thermal insulators, decreasing heat transfer between the ice and the coating [36].

2.2.1.7 Ice adhesion

There is considerable debate within the scientific community regarding the mechanisms and forces involved in the icing process. While most researchers recognize three main physical interactions contributing to ice adhesion to a solid—hydrogen bonding, van der Waals forces, and electrostatic interactions—the specific role of each remains a topic of discussion [37].

Some authors propose that electrostatic forces are the primary contributors to ice adhesion, suggesting that materials with low dielectric properties are better suited for achieving low ice adhesion strengths. Conversely, others argue that van der Waals forces primarily determine ice adhesion strength on solid surfaces. Some researchers attribute strong interactions between ice and solids to both van der Waals forces and electrostatic interactions, highlighting the significance of the electrical charge at the ice surface and the induced charge on the solid, making electrostatic interactions a dominant mechanism.

A more integrative perspective published by Farzaneh *et al* demonstrated that ice accumulation and adhesion result from a combination of the three aforementioned forces, along with mechanical adhesion due to the interlocking of water with surface features. Additionally, the chemical composition and environmental conditions are recognized as influential factors in ice adhesion interactions. The size and velocity of droplets, their angle of impact, and surface geometry also play crucial roles in ice adhesion and accretion [31, 38].

To quantitatively assess the ice adhesion of icephobic systems, researchers typically report values for ice adhesion strength to a surface, denoted as τ_{ice}. Icephobic materials are generally defined as those exhibiting $\tau_{ice} < 100$ kPa or $\tau_{ice} <$

20 kPa for passive systems, while materials like bare aluminum demonstrate $\tau_{ice} >$ 1000 kPa. Although the reported ice adhesion values are not directly comparable due to varying measurement conditions and often unique set-ups, they provide insight into material performance. Typically, materials or coatings with $\tau_{ice} < 100$ kPa are considered to exhibit potential icephobic performance [10].

A noteworthy and contrasting study by Tuteja *et al* focused on developing low interfacial toughness (LIT) materials. Unlike 'classic' icephobic materials, which rely on scaling performance with the iced area and are described primarily by τ_{ice}, LIT materials emphasize toughness. According to this concept, the force required to remove ice is independent of the iced area. Interfacial toughness quantifies the energy required for a crack at the interface to propagate, which is crucial for controlling delamination when the length of the interface is substantial [39, 40]. This distinction is significant for understanding ice adhesion measurements, as evaluating icephobic properties based solely on shear strength may provide an incomplete picture of a material's properties. As noted by the same authors, low interfacial shear strength does not necessarily imply low toughness; thus, the dynamics of removing ice at short interfaces may not directly translate to longer ones [39].

2.2.2 Limitations of superhydrophobic surfaces

The greatest challenge for icephobic materials is their need to perform effectively across various icing scenarios. Ice formation occurs under different temperature conditions, humidity levels, and wind conditions, resulting in diverse types of ice. It is well established that specific modifications to a material's roughness can achieve hydrophobic or superhydrophobic properties. However, there are limitations when these materials are intended for icephobic applications. Excessive roughness can negatively impact hydrophobic properties, potentially transforming the surface into a hydrophilic one. This transformation promotes increased water interaction with the surface and may enhance ice adhesion due to mechanical interlocking.

Mechanical interlocking is not limited to the static presence of water on a very rough surface. When water droplets impact a surface, they lose kinetic energy through spreading and retraction events. During the impact, two downward forces —wetting pressure and effective water hammer pressure—and one upward force, capillary pressure, are at play. If the sum of the downward forces exceeds the upward force, wetting occurs; otherwise, the droplets bounce off the surface. When droplets collide with high kinetic energy, the air pockets in the surface are displaced, leading to a Wenzel state. Under freezing conditions, the displacement of air pockets results in droplets with reduced mobility and an increased contact area, creating an ideal environment for ice nucleation to occur, followed by mechanical interlocking. Therefore, materials intended for icephobic applications should ideally maintain a constant Cassie–Baxter state during droplet collisions [32].

One significant limitation of these strategies is their reliance on wet chemistry for substrate coating. This often requires post-heating treatments, which may alter the polymeric and/or alloy structure or damage the substrate. In the study by Zeng *et al*, a detailed analysis of the contributions of wettability was conducted. Aluminum

samples were prepared through an etching method and then coated with PTFE [29]. To examine the effect of heterogeneous coated areas, spray-coated and dip-coated samples were compared. Despite having the same roughness, differences in icephobic properties were directly related to the heterogeneity of the coating technique. The freezing points were approximately −10 °C for the spray-coated sample and −26 °C for the dip-coated sample, highlighting the significant impact of the deposition technique on icephobic performance and underscoring the importance of achieving uniform coverage.

A promising alternative lies in initiated chemical vapor deposition (iCVD), a technique that allows for the synthesis and deposition of complex structures, such as graded, biolayer, or crosslinked coatings, with precise surface coverage and solvent-free synthesis. This method can effectively address the challenges of fluorinated compounds, which are of high interest but often limited by their solubility and compatibility with other molecules. By utilizing iCVD, the low chemical affinity and poor deposition adhesion of fluoropolymers can be managed effectively, leading to the development of new and promising structures for icephobic coatings [41].

2.3 Different functional chemistries

2.3.1 Silicone coated smooth substrates

Soft polysiloxanes are often selected as the base material for icephobic surfaces and coatings [42]. Their popularity in anti-icing applications stems not only from their chemically inert, non-toxic, non-flammable, and easily moldable nature but also from two key properties: softness and low surface energy. Silicones consist of an inorganic silicon-oxygen backbone, with two organic groups attached to each silicon atom in the main chain. The simplest and most common silicone material, polydimethylsiloxane (PDMS), has two methyl groups attached to the silicon atom in its repeating unit, as illustrated in table 2.1. With a Si–O backbone, silicone materials exhibit low intermolecular interactions, which result in low surface tension and surface energy. For instance, PDMS has a surface tension of approximately 20 mN m^{-1} at room temperature, whereas the corresponding surface tension for an aluminum substrate is around 500 mN m^{-1}. This low surface tension contributes to the water repellency and reduced ice adhesion strength of silicone materials. Given that the maximum water contact angle on smooth hydrophobic surfaces is 120°, PDMS, with a contact angle of approximately 110°, is considered one of the most hydrophobic surfaces among smooth substrates [10].

Although the water contact angles on polysiloxanes are not as high as those on superhydrophobic surfaces, silicone-based coatings can demonstrate extremely low ice adhesion strengths below 10 kPa. The icephobicity of polysiloxane is influenced not only by the wettability of the surface but also by the softness of the coating material. The Young's modulus of ice ranges from 0.3 to 3.6 GPa, while that of PDMS is less than 10 MPa. This significant difference in elastic moduli facilitates the removal of ice through DI. As shown in figure 2.4(a), even a small amount of stress can lead to the formation of cavities or cracks at the ice–substrate interface, thereby facilitating passive de-icing on the soft material [43, 44]. However, the DI

Table 2.1. Comparison of ice adhesion strength order and properties of common bulk polymers.

Polymer	Ice adhesion strength order[a]	Surface tension[b] (mN m^{-1})	Water contact[b] angle (°)	T_g[b] (°C)	Chemical structure
Polydimethylsiloxane (PDMS)	1	24	101	−123	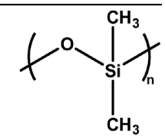
Polytetrafluoroethylene (PTFE)	2	18	108	−73	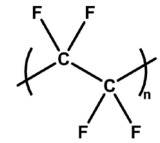
Low-density linear polyethylene (LDPE)	3	33	94	−130	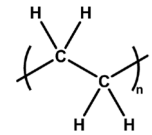
Atactic polypropylene (a-PP)	4	29	116	−10	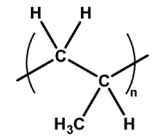
Polystyrene (PS)	5	33	91	95	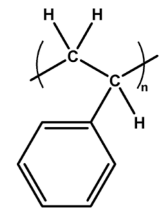
Polyvinyl chloride (PVC)	6	39	87	75	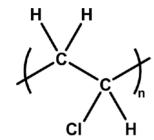

[a] Instead of giving specific values, the polymers are ordered from the lowest ice adhesion strength to the highest due to the lack of standards in ice adhesion measurements.
[b] The values have been obtained from [67].

mechanism alone is insufficient to reduce the adhesion strength of ice to PDMS significantly below 100 kPa [45]. There is a limit to how soft bulk silicone materials can be modified to achieve even lower ice adhesion strengths without compromising the mechanical durability of the surface. While optimizing the thickness of the coating can enhance its anti-icing performance, significant improvements require the combination of the hydrophobicity and softness of polysiloxanes with other innovative anti-icing strategies that can further reduce ice adhesion strength. The

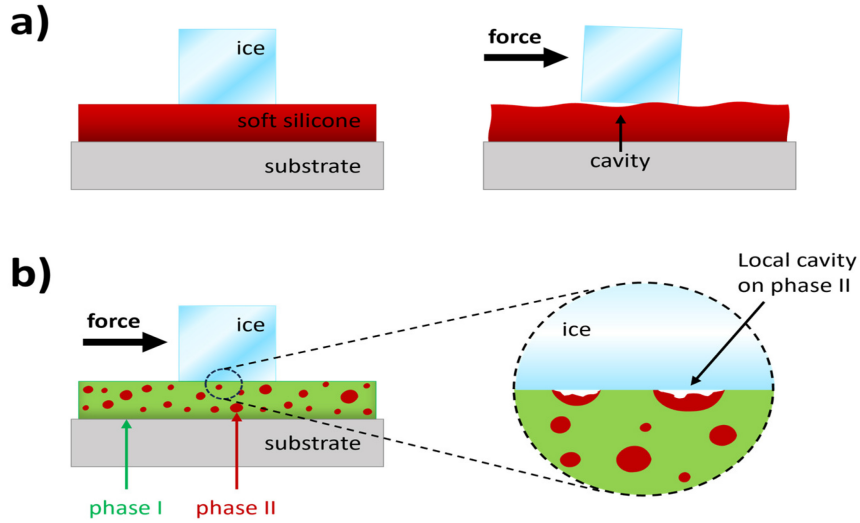

Figure 2.4. Soft silicone materials can be used to lower ice adhesion strength via DI. (a) An illustration of cavity formation in the ice–PDMS interface. (b) Illustration of a two-component polysiloxane coating with areas of high (phase I) and low stiffness (phase II). Crack formation in the softer phase results in remarkably easy ice removal.

lowest recorded ice adhesion strengths on polysiloxane materials were found on silicon elastomer coatings with distinct domains of a softer silicon-based organogel. This system, depicted in figure 2.4(b), utilized the notable difference in stiffness between the two phases to promote crack formation at the ice–coating interface. The resulting ice adhesion strengths achieved remarkable values, dropping below 1 kPa at their lowest.

2.3.2 Hydrated substrates

Another strategy for achieving icephobicity, which contrasts with the approach of increasing hydrophobicity, is to establish a stable layer of liquid water on the surface. In 2014, Dou *et al* developed durable anti-icing coatings that utilized an aqueous lubricating layer, significantly reducing the ice adhesion strength to the surface [46]. These coatings were formed from self-assembling amphiphilic block copolymers with a hydrophobic polyurethane (PU) backbone and pendant groups modified with hydrophilic dimethylolpropionic acid (DMPA). In this structure, the hydrophobic segments remained embedded within the coating, while the hydrophilic groups formed a hydrated corona on the surface. This hydrophilic corona had the capacity to absorb water, creating an aqueous layer that acted as a lubricant, smoothing out surface defects and minimizing mechanical interlocking between ice and the surface. Moreover, the charges on the pendant groups led to an increased ion concentration in the hydration layer. These ions contributed to a reduction in water activity and a lowering of the freezing temperature of the water [47]. In the study by Dou *et al*, the average ice adhesion strength to the coatings was measured

at 27 kPa, a sufficiently low value to allow wind speeds of 12 m s^{-1} to dislodge ice from the surface. The coating demonstrated resilience at temperatures as low as −53 °C, maintaining stable ice adhesion strength even after 30 icing/de-icing cycles [46].

Anti-icing surfaces employing similar lubricating water layers can remain effective even at extremely low sub-zero temperatures, depending on the type and quantity of ions incorporated into the hydrated layer. As illustrated in figure 2.5, hydrated anti-icing surfaces have been developed using ionizable or hydrophilic

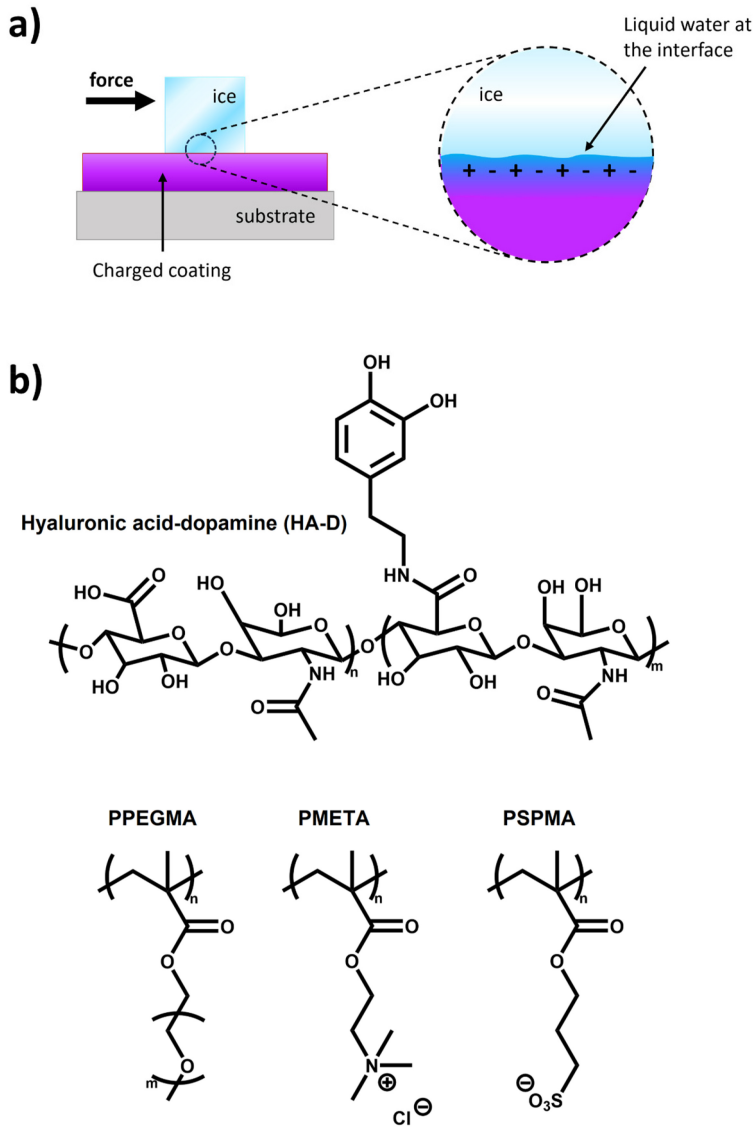

Figure 2.5. (a) An illustration of the interfacial lubricating water layer between the coating and ice. (b) Different functional chemistries for anti-icing via hydrated substrates.

polymeric chains, including hyaluronic acid (HA) [48], poly(acrylic acid) (PAA) [49], poly(ethylene oxide) (PEO) [50], poly(2-(methacryloyloxy)ethyl trimethylammonium) (PMETA) [51], poly(3-sulfopropyl methacrylate) (PSPMA) [58], poly(N,N-dimethylaminoethyl methacrylate) (PDMAEMA) [52], and poly(sulfobetaine methacrylate) (PSBMA) [53, 54]. Notably, these anti-icing coatings can also derive their lubricating layer from the ice itself; thus, evaporation of the water layer should not adversely affect the longevity of the surface. Once icing occurs, the interfacial water is replenished and remains effective as long as the ice persists atop the coating.

2.3.3 Polymer coated substrates

Since the mid-1900s, when the first studies on icephobic surfaces emerged, polymers have been the predominant material choice for anti-icing coatings. An article published in 1967 examined various commercially available plastics concerning their water contact angles and ice adhesion strengths [55]. Similar to polysiloxanes, the benefits of polymeric materials in anti-icing applications are largely attributed to their viscoelastic and hydrophobic properties.

Several soft polymers, beyond polysiloxanes, can effectively reduce ice adhesion strength via the DI mechanism. Bulk polymers characterized by minimal intermolecular interactions—such as the absence of polar groups, bulky side groups, and stereoregularity in the polymer chain—exhibit low glass transition temperatures (T_g) and low elastic moduli. Table 2.1 presents various common bulk polymers, ordered from the lowest to the highest ice adhesion strength. For instance, low-density polyethylene (LDPE) compares favorably to PDMS, with a surface tension of approximately 30 mN m^{-1}, a Young's modulus of 300 MPa, and an ice adhesion strength of 180 kPa. In the same experimental set-up, PDMS demonstrated a surface tension of 20 mN m^{-1}, a Young's modulus of 2 MPa, and an ice adhesion strength of 185 kPa [56].

Among all hydrophobic smooth coatings, perfluorinated polymers have consistently been the primary focus. Despite their higher T_g values and stronger hydrogen bonding with water compared to silicone materials, perfluorinated polymers generally exhibit slightly higher water contact angles. The water-repellent characteristics of these polymers arise from the small overall dipole moment of carbon-fluorine bonds, leading to low electrostatic interactions with water [57]. For instance, the average surface tension and water contact angle for polytetrafluoroethylene (PTFE) are 20 mN m^{-1} and 110°, respectively [58]. Additionally, perfluorinated polymers demonstrate excellent chemical resistance and thermal stability, owing to the stronger bond between carbon and fluorine compared to that between carbon and hydrogen. To address the mechanical durability issues associated with soft polysiloxane coatings, surfaces combining siloxane groups and perfluorinated polymer chains have been proposed. For example, a surface made of polymethyltrifluoropropylsiloxane (PMTFPS) along with polyacrylate copolymers showed improved anti-icing performance compared to the unmodified polyacrylate [59]. However, it is important to note that the measured ice adhesion strengths of around 300 kPa did not fall below the average values recorded for bare PTFE or PDMS.

2.3.4 Polymer brushes

The foundational studies for the development of polymer brush coatings with anti-icing properties date back several decades. In 1985, Murase and Nanishi [60] and again in 1994, Murase *et al* [61] reported the fabrication of an organopolysiloxane-based material containing Li^+ ions, which demonstrated very low ice adhesion strength. They attributed this finding to the presence of both bound and restrained water molecules, a result of the hydrogen bond disruption properties of Li^+ ions. However, these early investigations did not clarify the extent to which the incorporated ions within the polysiloxane matrix contributed to the material's anti-icing properties.

Years later, in 2014, Chernyy *et al* sought to further investigate this phenomenon and enhance understanding of how different counterions influence ice adhesion strength [62]. They prepared various surface-grafted polyelectrolyte brushes using surface-initiated atom-transfer radical polymerization (SI-ATRP) to allow controlled surface modification. The impact of ion incorporation within these polyelectrolyte brush layers on ice adhesion strength was systematically assessed with respect to well-defined surface chemistry.

From a chemical standpoint, five types of methacrylic monomers were polymerized on microscopic glass surfaces via SI-ATRP, enabling surface modification with functional groups such as oligo(ethylene glycol), sulfonate, quaternary ammonium, and carboxylate (as illustrated in figure 2.6). Coatings containing ionizable groups were further subjected to ion exchange to incorporate 13 mono-, bi-, and trivalent ions (H^+, Li^+, Na^+, K^+, Ag^+, Ca^{2+}, La^{3+}, CTA^+, F^-, Cl^-, BF_4^-, SO_4^{2-}, DS^-). The strongest kosmotropes, which are structure-making ions recognized for their significantly negative impact on water structural entropy (such as Li^+ and Na^+), were shown to reduce ice adhesion by 40% and 25%, respectively, at −18 °C. In contrast, no significant influence on ice adhesion was observed for weaker kosmotropes and chaotropes. At −10 °C, all polyelectrolyte coatings exhibited notable mitigation of ice adhesion, with reductions ranging from 20% to 80%, depending on the type of ion used.

He *et al* investigated heterogeneous ice nucleation on polyelectrolyte brush surfaces deposited on gold substrates [51]. The brushes consisted of densely end-grafted polyelectrolyte chains carrying a significant number of ionic groups, as illustrated in figure 2.7. The specific brushes utilized in the study included cationic poly[2-(methacryloyloxy)ethyl trimethylammonium] (PMETA) and anionic poly(3-sulfopropyl methacrylate) (PSPMA). In these brushes, the Cl^- in PMETA and K^+ in PSPMA could be exchanged for various counterions, such as SO_4^{2-}, F^-, acetate (Ac^-), HPO_4^{2-}, Cl^-, Ca^{2+}, Mg^{2+}, guanidinium (Gdm^+), K^+, and Na^+. When water droplets adhered to these polyelectrolyte brush surfaces, a portion of the counterions were released from the brushes due to osmotic pressure, forming a diffusion layer of counterions at the brush/water interface, as shown in figure 2.7. This created an ideal platform for investigating the ion-specific effects on ice nucleation on ionic surfaces. The study's findings indicated that heterogeneous ice nucleation could be modulated by exchanging the counterions of the polymer brushes. The distinct efficiencies of

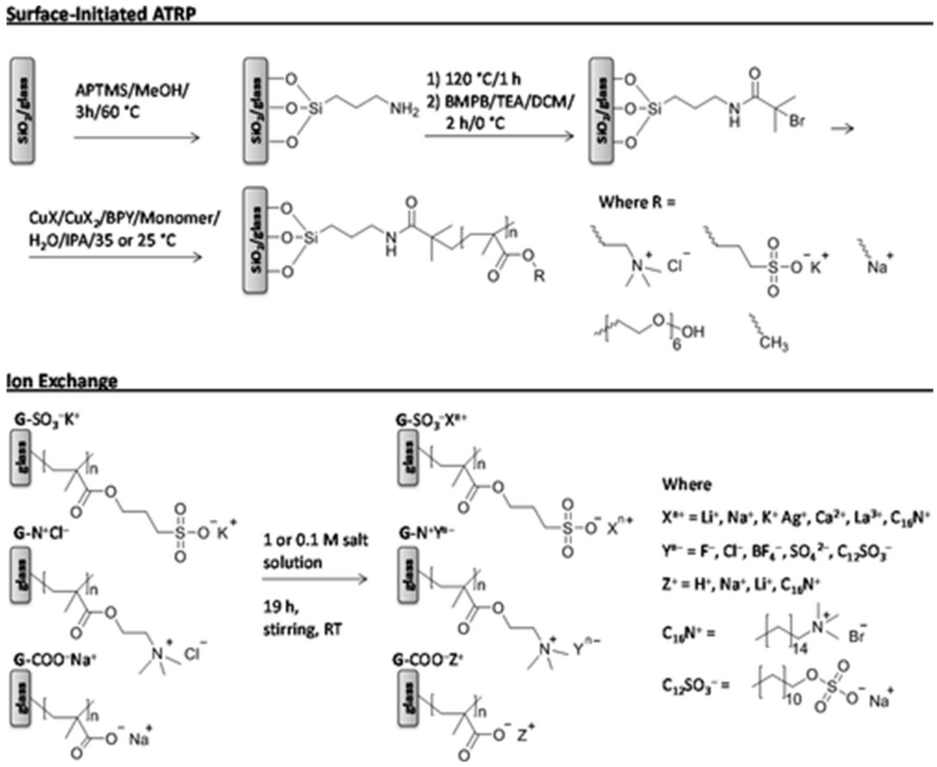

Figure 2.6. The graphical summary of undertaken experimental steps in the preparation of anti-icing polymer brushes using SI-ATRP, as reported by Chernyy *et al* [62]: A two-step solution-phase deposition was conducted involving (3-aminopropyl)trimethoxysilane (APTMS), followed by the reaction of the amine-terminated monolayer with 2-bromo-2-methylpropanoyl bromide (BMPB). Surface-initiated atom transfer radical polymerization (SI-ATRP) of a chosen monomer (KSPM [2], METAC [3], or NaMA [1]) was carried out using a catalyst system composed of CuX and CuX2 (X = Cl– or Br–), with a ligand (BPY) in a 1:1 H_2O/IPA mixture. Finally, the polyelectrolyte brushes were synthesized. (Adapted with permission from [62]. Copyright (2014) the American Physical Society.)

these ions in influencing heterogeneous ice nucleation followed the Hofmeister series. This phenomenon was further interpreted through molecular dynamics (MD) simulations, which demonstrated that the diffused counterions at the brush/water interface effectively regulated the dynamics and structure of the interfacial water, thereby influencing the heterogeneous ice nucleation (HIN) process.

Following the study focused on the ion-specific effects in heterogeneous ice nucleation on polyelectrolyte brush surfaces, the same group of researchers conducted an investigation on polyelectrolyte brush surfaces whose hydration was controllable through counterion exchange [52]. The results of this investigation revealed that ice propagation could also be tuned on the polymer brush surfaces by altering their hydration state. On highly hydrated polymer brush surfaces with hydrophilic counterions, ice propagation was facilitated due to the directional movement of trapped freezable water molecules towards the ice growth front. In

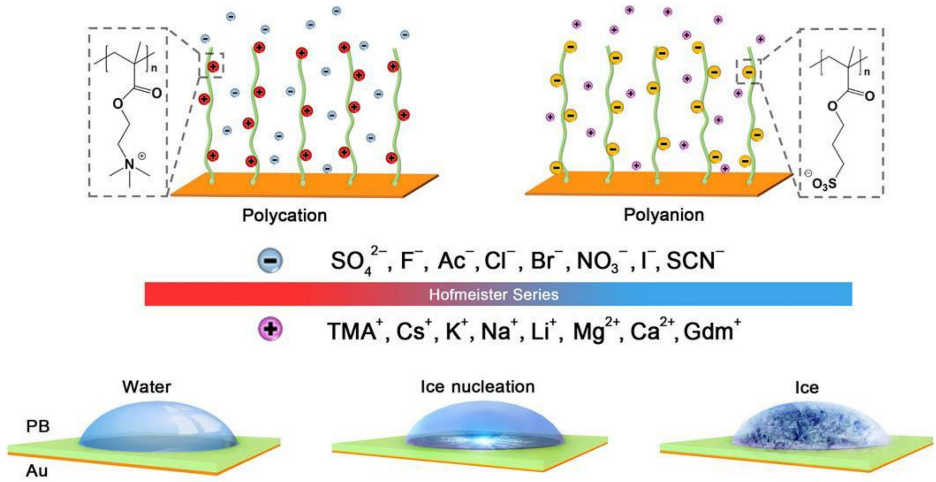

Figure 2.7. Illustration of heterogeneous ice nucleation on cationic and anionic polymer brush surfaces with different counterions based on the work by He *et al* [62]. Cationic poly[2-(methacryloyloxy)-ethyl trimethylammonium] (PMETA) and anionic poly(3-sulfopropyl methacrylate) (PSPMA) brushes have been used to investigate the effect of diffused counterions on tuning heterogeneous ice nucleation. The counterions on the PMETA and PSPMA brush surfaces were successfully exchanged by immersing the brush surfaces into a solution containing the desired counterions. (Reproduced with permission from [51]. Copyright (2016) AAAS.)

stark contrast, on dehydrated polymer brush surfaces with hydrophobic counterions, ice propagation was inhibited by the creation of a 'water depletion region' between droplets. The experimental results demonstrated that the difference in ice propagation rates could reach up to five orders of magnitude.

Liang *et al* prepared an anti-icing coating based on superhydrophilic polyzwitterion brushes [54]. They employed SI-ATRP to synthesize poly(sulfobetaine methacrylate) (PSBMA) brushes on silicon wafers, which are very flat and smooth substrates with easily controllable chemistry. The synthesis process of the SBMA polymer (PSBMA) brushes is illustrated in figure 2.8. In summary, a hydroxylated silicon surface was reacted with 2-bromo-2-methyl-N-[3-(trimethoxysilyl)propyl] propanamide (BrTMOS) as the initiator, forming a stable layer on the substrate that subsequently initiated the grafting polymerization of SBMA to create polyzwitterion brushes. The thickness of the PSBMA brush layers increased linearly with polymerization time, and a transition occurred from a nonassociated hydrophilic regime to a self-associated hydrophobic regime at a layer thickness of approximately 100 nm.

Thermal and chemical analyses revealed that PSBMA contained more nonfreezable bound water than typical polyelectrolytes, such as poly(sodium styrenesulfonate) and poly(2-(methacryloyloxy)ethyl trimethylammonium chloride), resulting in lower ice adhesion strength compared to the latter two. At −20 °C, the PSBMA brush coating exhibited a low ice adhesion strength of 60 kPa, indicating a significant reduction in ice adhesion by up to approximately 75% compared to uncoated silicon wafers. The optimum PSBMA layer thickness for achieving low ice

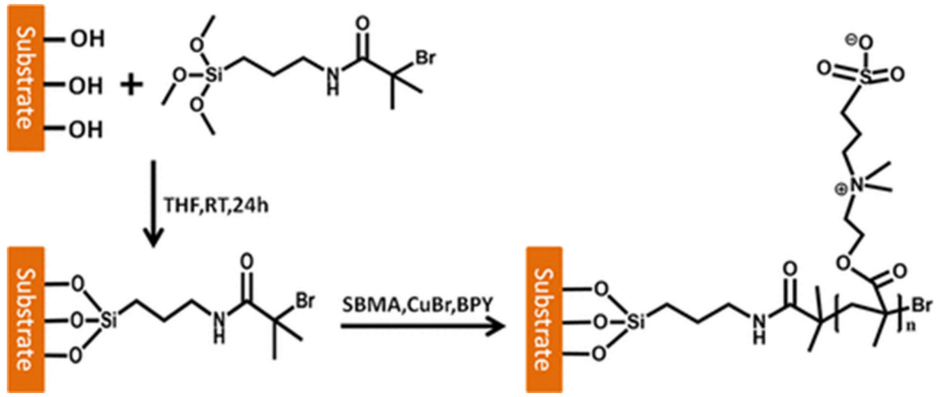

Figure 2.8. Synthesis of PSBMA polymer brushes through SI-ATRP polymerization on smooth silicon substrate based on the work done by Liang *et al* [54] (THF: tetrahydrofuran, RT: room temperature, BPY: 2,2′-bipyridine). (Adapted with permission from [54]. Copyright (2018) the American Physical Society.)

adhesion was found to be around 100 nm. These outcomes suggest that polyzwitterions are excellent candidates for anti-icing coating applications.

From the reviewed studies, it seems obvious that ions are involved in ice formations in various situations (e.g. in the anti-icing polymer brushes that are designed based on them). However, it is still not clear if there is an ion-specific effect of the heterogeneous ice nucleation. Accordingly, the field is extensively open for researchers to profoundly investigate new achievements in anti-icing polymer brushes based on ion-specific effects.

2.3.5 Slippery liquid infused porous surfaces

Generally, there are two types of natural-based anti-wetting surface designs that have inspired researchers. The first type is the traditional lotus leaf surfaces, which exhibit superhydrophobic characteristics due to the creation of air-infused micro- and nanostructured surfaces that minimize the contact area between the surface and liquid. While the underlying concept of this plant has proven effective in fabricating superhydrophobic surfaces, these structures have inherent drawbacks that adversely affect their efficacy in icephobic applications. Specifically, issues such as water condensation, frost formation, and increased ice adhesion arise from the loss of air voids within the porous structure under high humidity conditions. Condensed water domains can act as anchoring points for ice, facilitating its attachment to the surface upon freezing and leading to increased ice adhesion. Additionally, superhydrophobic surface designs are not easily scalable and face challenges under high-pressure impingement and high-temperature applications [63, 64].

The second nature-inspired concept for achieving anti-wetting surfaces addresses these drawbacks by utilizing lubricant-infused ‘slippery’ surfaces, which are inspired by the Nepenthes (tropical pitcher plants) [65, 66]. This unique characteristic of tropical pitcher plants was first investigated in 2004 [67], but the first adaptation of this feature in developing slippery liquid infused porous surfaces (SLIPSs) was

carried out in 2011 by Wong *et al* [66]. In their work, synthetic liquid-repellent surfaces were reported that consist of a film of lubricating liquid locked in place by a micro- and nanoporous substrate. The design principles behind their work include the following: (i) the liquid surface is intrinsically smooth and defect-free at the molecular level, (ii) it offers immediate self-repair by wicking into damaged areas of the underlying substrate, (iii) it is largely incompressible, and (iv) it can be tailored to repel immiscible liquids with virtually any surface tension. Their studies revealed that the developed SLIPS formed a smooth, stable interface that nearly eliminated the pinning of the liquid contact line for both high- and low-surface-tension liquids. Additionally, they minimized pressure-induced impalement into the porous structures, self-healed and maintained functionality after mechanical damage, and could even be made optically transparent. SLIPSs allow droplets to contact a layer of lubricant liquid rather than coming into intimate contact with the solid surface. This design results in several beneficial properties: a small sliding angle, low contact angle hysteresis, self-healing capability through capillary wicking upon damage, anti-icing ability, and strength to withstand external pressure [68]. The homogeneous and ultra-smooth nature of SLIPSs makes them particularly attractive for icephobicity (primarily passive anti-icing), as they reduce nucleation sites for ice and water on the surface. Consequently, even if water droplets condense on an SLIPS, they can readily roll off due to the remarkably low contact angle hysteresis [69].

Over the years, significant efforts have been made to optimize the originally developed SLIPSs for icephobicity, resulting in considerable advancements in the field. Heydarian *et al* have categorized SLIPSs into two main groups [70], lubricated micro/nanotextured surfaces and oil-infused polymeric systems. The first category is further divided into two subcategories: ordered textured surfaces and disordered textured surfaces. Various methods have been developed for fabricating SLIPSs, including layer-by-layer (LbL) assembly [71, 72], liquid flame spray (LFS) [73, 74], templating [75, 76], laser lithography [77, 78], and spray and spin methods [79, 80], as well as the creation of magnetic slippery surfaces [81, 82]. Recent studies continue to contribute to the SLIPS field, either focusing on their individual operation or in combination with other anti-/de-icing features. For instance, Liu *et al* combined 'oil film isolating' with electric heating coatings to create a reliable and durable anti-icing coating [83]. To enhance the immobilization of the oil film, they proposed a convenient self-assembly method for constructing closely aligned micropores on the electric heating coating. This approach resulted in a slippery property for the porous electric heating coating after infusing silicone oil into the semi-closed porous structures. A brief description of this method and its steps are illustrated in figure 2.9. More recently, we (Singh *et al*) have shown the use of reticular materials, metal–organic frameworks (MOF) in enhancing the stability of SLIPSs which exhibited excellent anti-icing performance [84].

Cheng *et al* developed a method to prepare photo-thermal slippery surfaces (PSSs) that demonstrate rapid self-repair, exceptional anti-icing and de-icing performance, and excellent stability [85]. These PSSs are created by combining a cost-effective photo-thermal conversion material (black paint), a solid lubricant (paraffin wax), and a porous polyamide (PA) substrate. For instance, the PSSs can

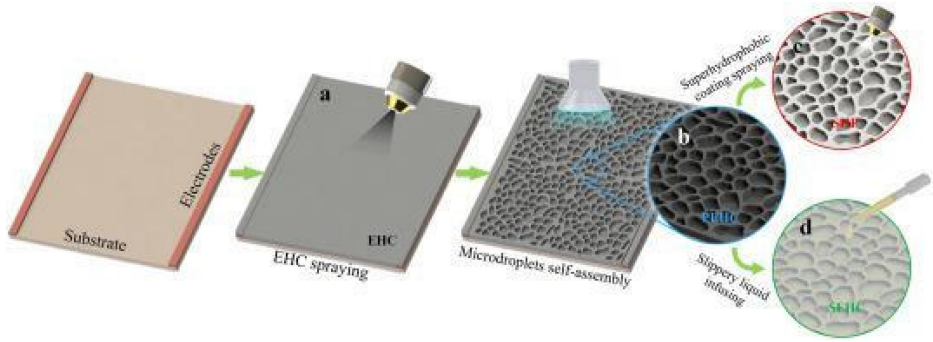

Figure 2.9. Fabrication of the porous electric heating coatings with different functions: (a) smooth electric heating coating (EHC), (b) EHC with close-aligned micropores (PEHC), (c) hydrophobic silica sprayed PEHC (SHP), and (d) slippery silicone oil-infused PEHC (SEHC). (Adapted with permission from [83]. Copyright (2019) Elsevier.)

rapidly self-repair under 1 sun illumination when the surface temperature exceeds 12 °C ± 1.0 °C or under near-infrared (NIR, 808 nm, 300 mW cm^{-12}) when the temperature is higher than –20 °C ± 1.0 °C. Furthermore, at temperatures above –12 °C ± 1.0 °C, ice formation is prevented on the PSSs under 1 sun. Even at lower temperatures, down to –20 °C ± 1.0 °C, ice formation is delayed, taking 212.5 ± 2.5 s to occur.

Despite the advantages of SLIPSs in anti-icing applications, their durability can be compromised, leading to failure in certain operational conditions. SLIPSs achieve liquid repellency primarily through the immiscibility of the lubricants used. A low surface energy lubricant is infused into the surface structure, creating an interface with the immiscible working fluids that results in very low contact angle hysteresis. For effective performance, three criteria must be satisfied: (a) the solid substrate must have a higher affinity for the lubricant than for the droplet; (b) the lubricant and the working fluid must be immiscible; and (c) the lubricant must wick into, spread, and adhere stably within the structure. The primary source of failure for SLIPSs is their inability to retain the lubricant, leading to drainage of the lubricant layer and causing contact line pinning of the working fluid on exposed solid structures [86, 87]. Addressing durability issues and other drawbacks of SLIPSs often requires careful selection of materials, and several studies have been conducted in this regard [84]. The durability of icephobic materials presents a paradox: while they are engineered to prevent ice adhesion and formation, their effectiveness frequently diminishes under prolonged or extreme weather conditions, precisely when such properties are most critical [88–90].

To address the challenges associated with ice adhesion, a new class of ‘smart’ icephobic coatings has emerged, integrating functionalities such as self-lubrication and phase change materials (PCMs) [91]. PCMs present an innovative solution by undergoing phase transitions that either absorb or release latent heat, thereby counteracting ice formation [92]. While PCMs have been utilized in various applications—including solar panels [93], building materials [94], electronics [95],

and road surfaces [96]—their potential in anti-icing coatings remains relatively underexplored [97]. Encapsulated PCMs (EPCMs) offer an effective means of stabilizing these materials by embedding them within protective shells that prevent leakage and facilitate controlled heat release [98]. This encapsulation, typically achieved through micro-encapsulation, creates a barrier around the PCM core, making it easier to integrate into a matrix, which enhances durability during multiple icing cycles (as illustrated in figure 2.10). Recent innovations, such as PCM-impregnated porous metallic structures (PIPMSs), further enhance the icephobic capabilities of SLIPSs by incorporating solid lubricants such as polyethylene glycol (PEG) or coconut oil into the porous matrix [99]. This combination addresses the challenge of lubricant loss, achieving ultra-low ice adhesion (<5 kPa) and withstanding up to 50 icing/de-icing cycles with minimal depletion of the PCM. By releasing latent heat and maintaining a lubricated interface, these materials not only delay ice formation but also support long-term durability in challenging environments. In summary, the integration of EPCMs with various other icephobic coatings —including self-lubricating, photo-thermal, polymeric matrices, and porous metallic substrates—bridges traditional PCM applications with innovative anti-icing needs, offering a promising solution for resilient icephobic surfaces.

2.3.6 Photo-thermal materials

Electro-thermal de-icing has emerged as one of the most widely investigated active de-icing strategies, garnering attention from numerous researchers. This method employs Joule heating, which arises from electrical resistivity, to mitigate ice adhesion and accretion on surfaces [100]. In this approach, a conductive coating layer is deposited onto the surface, and a voltage difference is applied. The resulting flow of electrical current generates heat through the frictional resistance encountered

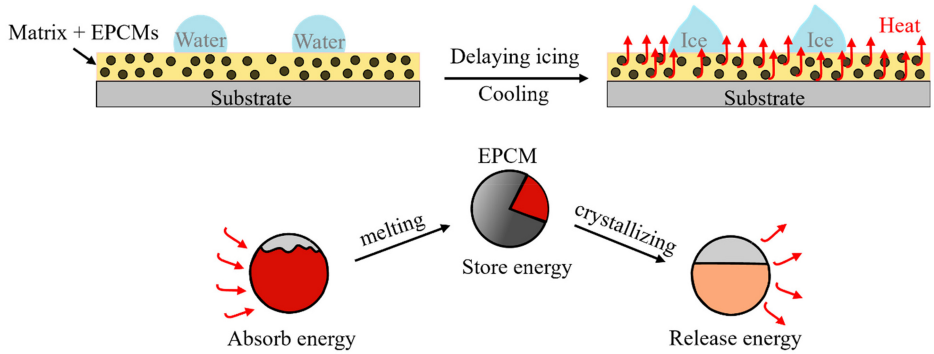

Figure 2.10. Schematic representation of the phase change materials incorporated into a matrix. The (black) shell encapsulated the core (red) functional material, in this case the PCM, enhancing its durability and thermal properties. The material matrix (yellow), in this case a slippery liquid infused porous surface, works as a binder to hold the EPCMs in place while enhances its anti-icing properties. The EPCM working principle relies on absorbing, storing, and releasing energy as heat. EPCMs absorb energy (melt of PCM) from various factors such as outdoor temperature, active heating system etc. When temperatures drop, the stored energy is released (crystallization of PCM) to delay ice formation.

by electrons as they move through the material. This internal heating effectively melts the ice, facilitating de-icing. Despite its advantages, a significant drawback of electro-thermal de-icing is the high energy consumption associated with heat production. To address this challenge, researchers have explored alternative methods that offer greater efficiency, such as surfaces and coatings with photo-thermal effects that convert solar illumination into heat [101].

A pioneering study by Dash *et al* [102] introduced photo-thermal 'traps' designed to mitigate icing. These traps, which are laminates applied to a base substrate, enhance de-icing by converting solar illumination into heat at the interface between the ice and the substrate. The underlying mechanism involves three complementary layers (as depicted in figure 2.11): a selective absorber for solar radiation, a thermal spreader for lateral heat dispersal, and an insulation layer to minimize transverse heat loss.

Upon illumination, the thermal confinement created at the heat spreader results in a rapid increase in surface temperature, leading to the formation of a thin lubricating melt layer that facilitates the removal of ice. According to the findings of this study, solar illumination can induce a temperature increase of up to 33 °C, making this de-icing method highly energy-efficient

Mitridis *et al* [100] proposed metasurfaces with embedded plasmonically enhanced light absorption heating by means of ultrathin hybrid metal-dielectric coatings, acting as a passive and facile strategy for simultaneous de-icing and anti-icing effects solely based on solar illumination as the energy source. In this method, surface transparency is a must and the balance between transparency and absorption is attained by rationally nanoengineered coatings consisting of gold nanoparticle inclusions in a dielectric (titanium dioxide), in which the broadband absorbed solar energy is concentrated into a small volume. As a consequence, a more than 10 °C temperature rise happens in relation to the ambient air at the air–solid interface, which is the place of most ice formation. This leads to retarding water freezing and

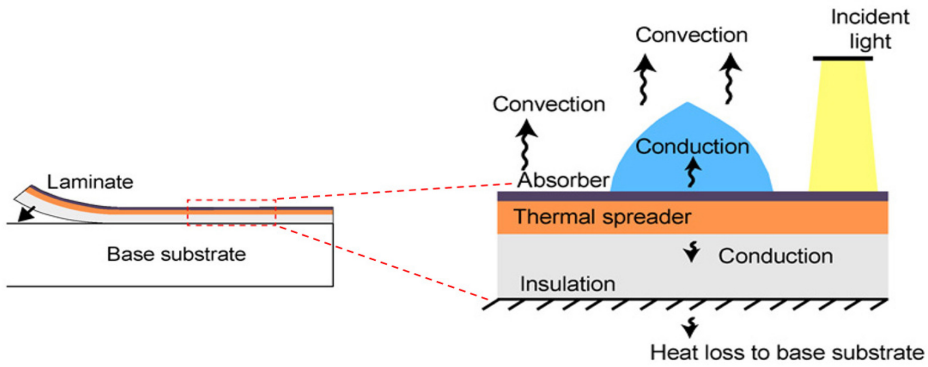

Figure 2.11. Schematic representation of the photo-thermal trap designed by Dash *et al* applied on the base substrate as a laminate and the attributed heat transfer mechanisms. The laminate consists of (top to bottom) highly absorbing cermet, thermal spreader, and insulating layer. (Reproduced with permission from [102]. Copyright (2018) AAAS.)

mitigating ice adhesion (when it occurs) and hence, obtaining anti/de-icing concurrently.

Wu *et al* [103] have employed candle soot to fabricate superhydrophobic photo-thermal icephobic surfaces with high photo-thermal efficiency. The designed coating solution for attaining the photo-thermal icephobic surface consisted of three components as candle soot, silica shell, and grafted PDMS brushes. Candle soot, as an inexpensive material, has been able to provide hierarchical nano/micro-structures capable of trapping sunlight in order to improve light absorption resulting in high photo-thermal efficiency. Also, silica shell was used to strengthen the hierarchical candle soot, and grafted PDMS (as a low-surface-energy material) brushes endowed the surface with superhydrophobicity. When assessing the photo-thermal performance, it has been observed that upon illumination under 1 sun, the surface temperature could increase by 53 °C. This per se could indicate no ice formation at environmental temperature to as low as −50 °C, and the fabricated coating system was able to promptly melt the accumulated frost and ice in 300 s. The photo-thermal feature was even more promoted by superhydrophobicity. In this regard, the superhydrophobic candle soot surface could eliminate the melted water instantly, leaving a dry surface behind, which prevented the accumulation of melted water and thus decreased the heat loss. Second, the surface benefited from self-cleaning, therefore, dust and other contaminants could be wiped away by rain or melted water and the chance of blocking sunlight exposure was minimized. According to the authors' report, the designed photo-thermal icephobic surface, as shown in figure 2.12, exhibited outstanding potential and broad impacts thanks to its cheap base materials, simplicity, eco-friendliness, and high energy efficiency.

Wu *et al* [101] developed hierarchically structured PDMS/reduced graphene oxide (rGO) films that demonstrate excellent anti-icing and de-icing performance. Their study focused on creating crosslinked PDMS/rGO films that can effectively adsorb and convert solar energy for *in situ* de-icing, facilitated by the incorporation of dispersed rGO sheets within the PDMS networks. An diagram of the processes undertaken is provided in figure 2.13(a). The researchers employed two templating methods: an emulsion template to produce porous PDMS/rGO (EPG) films and a sugar/salt template for PDMS/rGO (SPG) films. They further utilized a one-pot dual-template technique to fabricate hierarchically structured PDMS/rGO (HPG) films. The resulting multi-hierarchical-structured surfaces exhibited efficient broad-band solar light absorption and high energy transfer efficiency of 90.4%. This efficiency is attributed to the presence of pores with diameters in the hundreds of microns, as well as micro-scale wrinkles on the internal walls, which create additional traps and longer trajectories for incident light (as shown in figure 2.13(b)).

The findings revealed that films containing 0.3 wt% rGO maintained surface equilibrium temperatures above freezing, even at −40 °C, allowing for easy ice removal under 1 sun illumination. These films demonstrated high de-icing efficiencies across various simulated realistic conditions, highlighting their effectiveness in diverse geographical settings, where available solar illumination can vary significantly based on location, climate, and weather conditions.

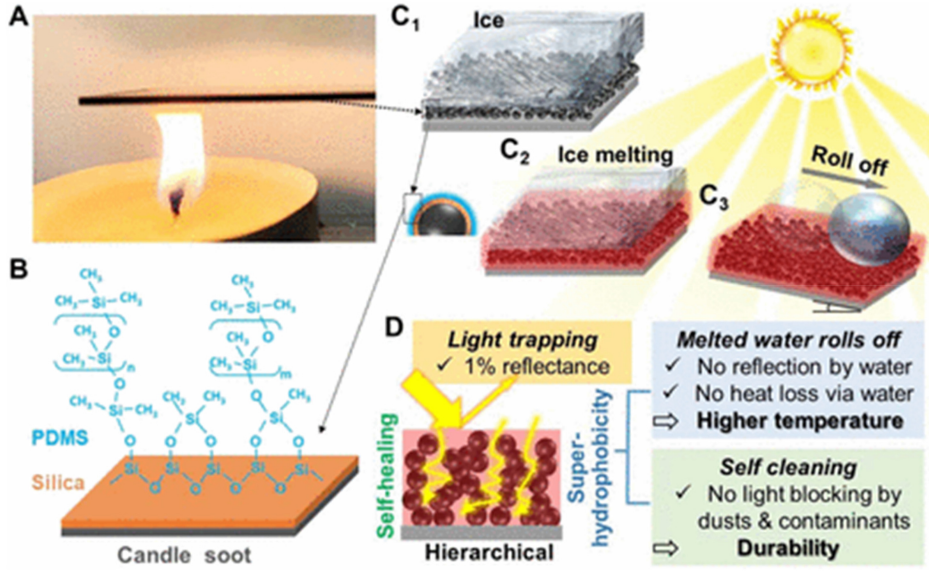

Figure 2.12. Schematic representation of the icephobic surface and fabrication process according to Wu *et al* [103]. (A) Candle soot is deposited onto a glass slide positioned above the candle flame. (B) Structures of the soot particles after being coated with a silica shell, followed by the application of PDMS brushes. (C) Mechanism of the proposed icephobic surface: Under sunlight exposure, the accumulated ice on the surface (C1) melts due to heat generated by the photo-thermal effect (C2), and the melted water then rolls off the inclined surface (C3). (D) The hierarchical structures enhance the surface with light-trapping properties and superhydrophobicity. (Adapted with permission from [103].)

The authors concluded that the advantages of this icephobic system—its broad applicability on a variety of substrates, excellent durability, and low cost—position it as a promising candidate for practical long-term applications in ice management.

In the study by Xie *et al* [104], researchers combined photo-thermal conversion with superhydrophobic materials to achieve exceptional anti-icing and photo-thermal de-icing performance. They developed a carbon-nanowire array on carbon cloth using an electrochemical deposition method, followed by a silanization treatment to create carbon-based materials with micro–nano hierarchical structures. These structures exhibited high-performance photo-thermal superhydrophobic anti-icing and de-icing capabilities, as illustrated in figure 2.14. The results demonstrated that the dense carbon-nanowire array on the surface of the micron carbon fiber provided excellent superhydrophobicity while enhancing light absorption due to the trapping effect induced by the hierarchical structure. The water contact angle measured on the prepared surface reached 155°, and under a solar power density of 1 sun, the temperature increased rapidly to 90 °C. Additionally, the air trapped within the micro–nano hierarchical structures effectively inhibited heat transfer during the icing process, resulting in a significant increase in the icing delay time from 241.22 to 3517.33 s under low-temperature conditions. These findings confirmed the remarkable photo-thermal conversion properties of the developed

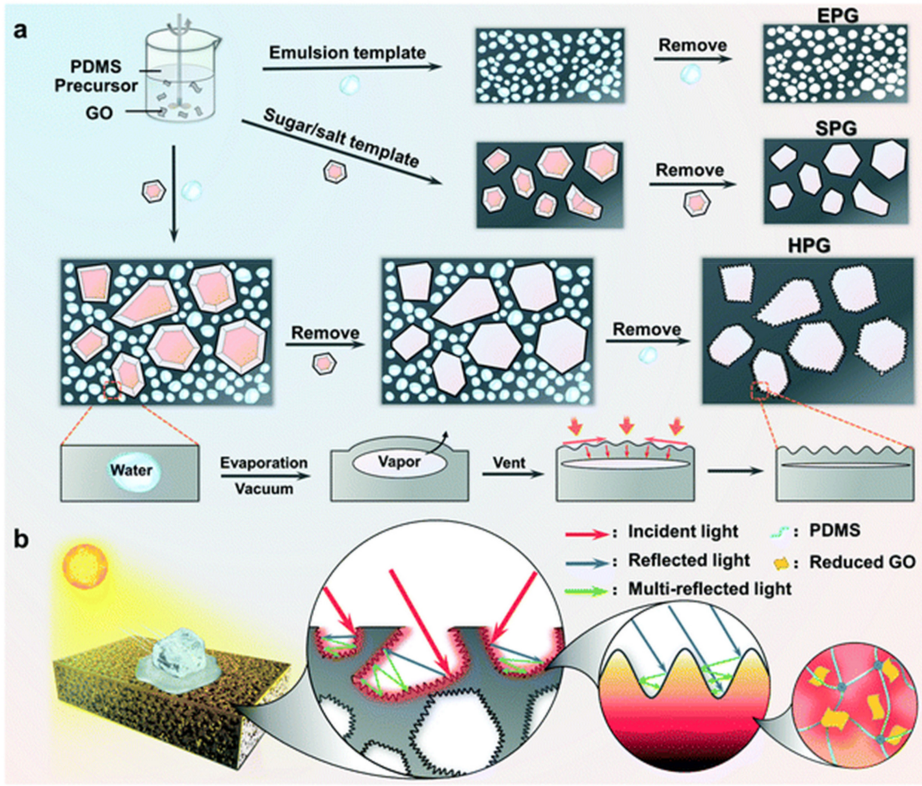

Figure 2.13. (a) Fabrication of porous emulsion-templated PDMS/rGO (EPG), sugar/salt-templated PDMS/rGO (SPG), and hierarchical-structured PDMS/rGO (HPG) films. (b) Schematic illustration of the solar anti-icing/de-icing performance of the HPG film. The dual-scale hierarchical macrostructures promote multiple internal reflections, thereby improving solar-to-heat conversion efficiency. (Adapted with permission from [101]. Copyright (2020) Royal Society of Chemistry.)

surfaces, showcasing their potential for photo-thermal de-icing. The authors propose this method as a promising approach for the next generation of de-icing and anti-icing materials, capitalizing on the benefits of low cost, durability, high-efficiency photo-thermal conversion, and excellent superhydrophobic performance.

Overall, de/anti-icing strategies based on photo-thermal materials and their effects are rather newly investigated and there are a lot of knowledge gaps and open-to-investigate details for future studies in order to verify the existing outcomes and optimizations.

2.4 Combining surface chemistry with additional mechanisms

2.4.1 Nanoscale carbon coatings

Various strategies have been explored utilizing carbon nanotubes (CNTs) and graphene as coatings, which exhibit superhydrophobic properties beneficial for

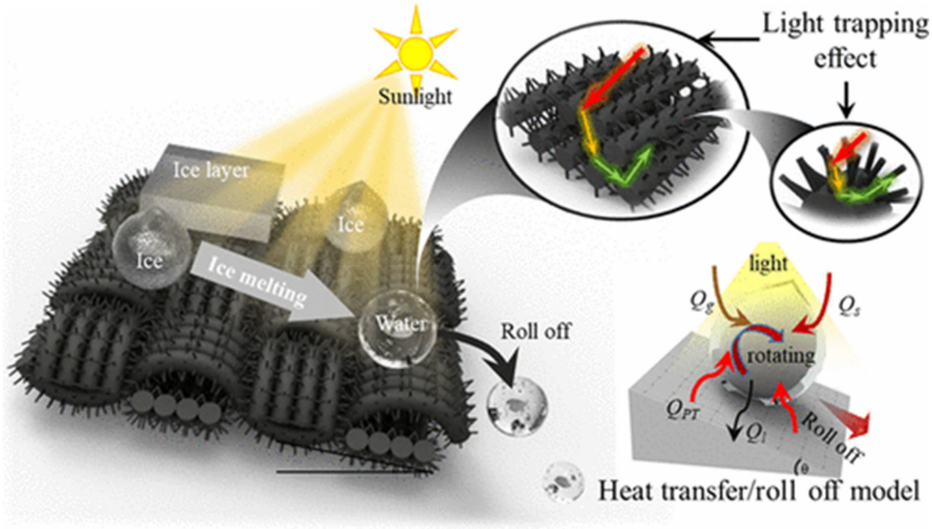

Figure 2.14. Carbon-based materials with micro–nano hierarchical structures with high-performance photothermal superhydrophobic anti-icing/de-icing features. (Adapted with permission from [104]. Copyright (2021) American Chemical Society.)

icephobic applications. These coatings not only provide mechanical durability but also enhance electrical properties [35]. The production of carbon nano-films is relatively simple and cost-effective. In a study by Yao *et al*, icephobic amorphous carbon nano-films were fabricated using ethanol-flame synthesis. These coatings featured multiple micro-textures, achieving a water contact angle of 155° and a sliding-off angle of 5° (figures 2.15(a) and (b)). The icephobic characteristics of the films were evaluated through various experiments, assessing parameters such as freezing time, ice adhesion strength, and dynamic sliding-off angles of droplets [105]. Similarly, Miller *et al* presented an approach involving fluorinated carbon films deposited via a deep reactive ion etching system. To investigate the effect of surface roughness, certain substrates were sandblasted to create textural features prior to film deposition. Their findings indicated a correlation between water contact angles and ice adhesion strength for samples with comparable roughness [108]. Additionally, a composite of graphene nanoribbon (GNR) stacks and epoxy was developed by filling epoxy with GNR stacks. This composite resulted in a conductive polymer suitable for use in de-icing systems, particularly in the aircraft industry [109]. Tour *et al* also employed GNRs in a de-icing heating layer composite, aimed at protecting radio-frequency equipment (figure 2.15(d)) [107]. Later, the same research group introduced an innovative strategy using perfluorododecylated graphene nanoribbons (FDO-GNR). They designed films that function for anti-icing purposes, which can switch to a slippery de-icing mode when lubricants are applied. These films are spray-coated, enabling large-scale manufacturing (figure 2.15(c)) [106].

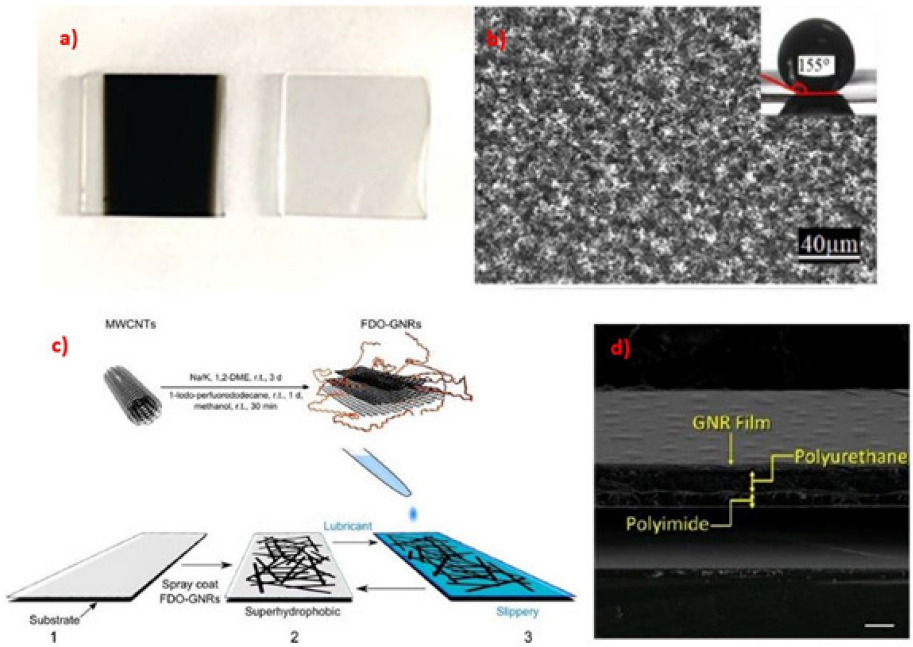

Figure 2.15. (a) Glass substrate with and without carbon nano-film. (b) SEM image of the carbon nano-film. (c) Representation of FDO-GNR synthesis and fabrication of FDO-GNR films. (d) SEM image of the GNR film. The system consists of a polyimide on the bottom, the clear-coat Dulpli-color automotive paint in the middle, and the GNR film as the upper layer. ((a) and (b) Adapted with permission from [105]. Copyright (2019) Elsevier. (c) Adapted with permission from [109]. Copyright (2016) American Chemical Society. (d) Adapted with permission from [108]. Copyright (2014) American Chemical Society.)

2.4.2 Anti-freeze proteins

Observing nature provides valuable insights for developing systems that maintain their properties in cold environments. Numerous living organisms, including plants and animals, exhibit remarkable resilience to cold temperatures, adapting to temperature fluctuations through complex mechanisms involving multiple variables. While these natural adaptations are intricate and challenging to replicate, they serve as a foundation for designing simpler systems to mitigate and delay ice formation.

One significant area of study is the existence of ice-binding proteins (IBPs), which bind to ice and modify its structure. Among these are antifreeze proteins (AFPs), which interact with ice crystals to alter their shape and control ice formation. These properties are crucial for the survival of many organisms in frigid habitats. Although the precise mechanisms by which AFPs operate are still under investigation, the most widely accepted theory is the adsorption-inhibition mechanism. This mechanism posits that AFPs inhibit ice growth by nano-confining water molecules, limiting their movement and preventing them from organizing into ice crystals. This process accounts for two important effects in delaying freezing: thermal

hysteresis (TH), which lowers the freezing temperature below the melting point, and ice recrystallization inhibition (IRI), which helps regulate the size of ice crystals.

The physical properties and states of condensation can vary significantly with confinement dimensions, temperature, pressure, and interactions with surfaces. Research suggests that the coexistence of spatially segregated hydrophobic and hydrophilic domains is crucial for delaying water freezing [110]. Successful attempts have been made to create anti-icing surfaces on solid substrates such as aluminum [111] and glass [112] by incorporating AFPs, resulting in decreased supercooling before water freezes on the surface or reduced frost growth. However, challenges remain, including the difficulties associated with the extraction of AFPs, which can drive up material costs, and the limited long-term stability of these proteins, often only lasting a few days on glass [113].

While replicating such complex biological systems in practical applications poses significant challenges, leveraging the fundamental principles behind these mechanisms offers a promising avenue for innovation. Hydrogels, for instance, present interesting opportunities. The properties of hydrogels can be finely tuned through chemical modifications, allowing control over the interfacial regions, water content, and mobility. This tunability makes hydrogels a useful platform for designing bio-inspired strategies to control the organization of water molecules in a system.

In particular, organohydrogels—composed of classical hydrogels infused with an oil phase—offer a promising approach to integrate materials that exhibit anti-icing properties by adjusting the characteristics of interfacial water [114]. In these systems, solvents or ionic compounds can be incorporated between polymer networks, providing a wide range of modifications to inhibit the formation of crystalline water structures [115]. This approach utilizes the concepts developed by AFPs while avoiding the challenges associated with using the proteins themselves. Section 2.4.5 will delve into the chemistries and applications of hydrogels and ionogels in anti-icing strategies in more detail.

2.4.3 Wettable polymeric coatings

Many studies in the past have documented a correlation between high water contact angles and lower ice adhesion strengths [57, 116–118]. In 2010, Meuler *et al* connected these two variables via equation (2.6) which predicts the value of ice adhesion strength τ_{ice} from the receding water contact angle θ_{rec} of a substrate [117]. Hence, research in the field was for a long time focused on maximizing water-repellent properties in order to reach the lowest possible ice adhesion strength to a surface. As the limitations of SHS have become more evident, the field has started to accept that a high water contact angle does not guarantee icephobicity of a surface [119–122].

In some cases, smooth hydrophilic surfaces, such as silicon wafers, have shown lower ice adhesion strengths and higher freezing delay times compared to their hydrophobic and/or superhydrophobic counterparts in the same study [119, 120]. More notable is, however, the appearance of the first hydrated surfaces in 2014 [46, 48]. These wettable coatings with a continuous layer of water on top have proven to

be able to reduce ice adhesion strength down to the scale of 10 kPa while simultaneously staying functional in record-breaking low temperatures. It has also been observed that polymers with flexible mobile chains on the surface of the material induce interfacial slippage that can reduce ice adhesion strength to below 1 kPa [10]. In the work of Golovin *et al*, several elastomers were embedded with mobile polymer chains or oils to study the effect of crosslink density and interfacial slippage on the ice adhesion and durability of the polymer substrates. Although most of the samples were hydrophobic fluorinated or silicone-based elastomers, remarkably, a series of hydrophilic oil embedded PU rubbers showed the lowest ice adhesion strength with values below 10 kPa:

$$\tau_{ice} = \beta\gamma(1 + \cos(\theta_{rec})). \tag{2.6}$$

In equation (2.6), β is an experimental constant and γ is the surface tension of water.

2.4.4 Non-wettable polymeric coatings

Major classes of non-wettable polymers reported for anti-icing applications are outlined in this section.

2.4.4.1 Fluorinated materials

Fluorinated polymers account for the most commonly and widely studied classes of anti-icing materials. The high content of $-CF_3$ groups in their structures, results in remarkably low surface energy, much lower than liquid water (<72 mN m^{-1}), and consequently fluorinated materials constitute candidates for anti-icing applications. The capability of poly(tetrafluoroethylene) to act as icephobic material has been systematically studied. The hydroxyl groups present on the oxide surfaces (i.e. Al_2O_3, SiO_2, TiO_2) or metals, are capable of reacting with functional groups of molecules, making them good substrates to obtain fluorinated materials. At the same time, the group orientation has attracted much attention. Yang *et al* reported that ice adhesion on a bare Al surface was measured at $\sim$1500 kPa. Both smooth and rough fluorinated surfaces were found to have very little ice adhesion, namely $\sim$100 and 200 kPa if compared to bare Al. The ice accretion is minimal on very high morphological non-homogeneities, such as micrometric porous superhydrophobic polyvinylidene fluoride (PVDF), due to the low adhesion and limited contact area between the water drops and coating.

Although morphology plays a critical role, good anti-icing properties have also been obtained by orienting fluorinated functionalizing groups. By covalently bonding the functionalized fluorinated molecules to the surface of the substrate, it is possible to form monolayers of self-assembling molecules (figure 2.16). In that way, by orienting fluorinated or other hydrophobic groups with low free energy groups in the desired direction, particularly towards the water interface, the water repellency effect is maximized and ice adhesion strength is decreased [123].

Recently, Chen *et al* fabricated an anti-icing coating capable of tolerating extreme environmental conditions, such as ultra-low or high temperatures, strong acids or alkalis and long-term exposure to sunlight. This coating is developed by

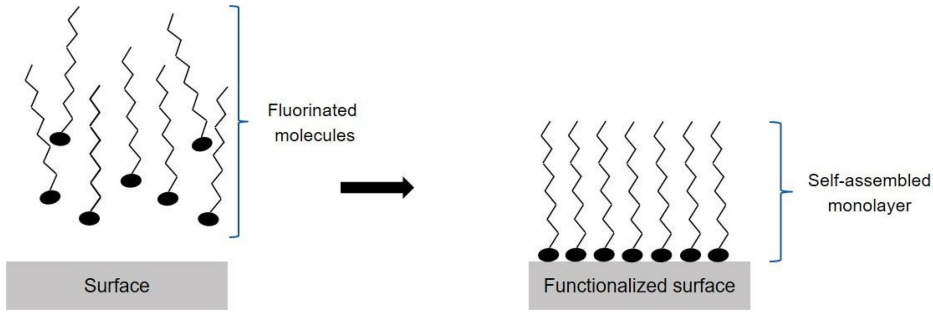

Figure 2.16. Self-assembly of functionalized molecules forming a monolayer on a solid surface.

incorporation of fluorinated amphiphilic copolymers (PFA-PVP-PDMS) and photo-thermal nanocarbon fibers (NFs), which transfuse the de-icing properties to the coating, into a PDMS matrix. It is very important that both the morphology and the de-icing performance are maintained after exposure to extreme environmental conditions, attributable to the tough coating materials and the intrinsic anti-icing properties of materials rather than artificial surface structure.

2.4.4.2 Non-fluorinated materials

Fluorine-free materials are increasingly recognized for their environmental benefits, leading to a surge of interest in recent years. Consequently, many researchers have focused on developing low-cost, eco-friendly preparation techniques for producing fluorine-free hydrophobic coatings, which hold significant potential for large-area applications, particularly in outdoor settings such as anti-icing surfaces.

Xie *et al* reported a facile spray-coating approach for the fabrication of non-fluorinated and durable anti-icing superhydrophobic coating by the combination of an aqueous suspension of hexadecyl polysiloxane, prepared by hydrolytic condensation of hexadecyltrimethoxysilane (HDTMS, 98%) and tetraethoxysilane (TEOS, 99.9%) onto the DE microparticles in water. These microparticles were modified by natural diatomaceous earth (DE@HD-POS) and a waterborne PU aqueous solution. The PU/DE@HD-POS coatings showed excellent superhydrophobicity with a high contact angle and a low sliding angle. The coatings demonstrated robust mechanical stability while exhibiting outstanding anti-icing performance, characterized by notably longer freezing times and reduced ice adhesion strength on diverse substrates substrates [124].

Xie *et al*, in another study, described non-fluorinated and durable photo-thermal superhydrophobic coatings based on natural attapulgite nanorods for efficient anti-icing and de-icing. A coating consisting of oxidative polymerized polypyrrole and hydrolytically condesated hexadecyl polysiloxane was formed on the attapulgite nanorods. The photo-thermal superhydrophobic coatings were deposited by spray-coating. The coatings demonstrated excellent superhydrophobicity due to the highly hierarchical micro-/nanostructure and the low surface energy. Moreover, the coatings showed good mechanical, chemical and thermal stability [125].

Wu *et al* presented transparent, fluorine-free, and antireflective hydrophobic coating created via the hydrolysis of TEOS combined with the hydrophobic modification of methyl MQ silicone resin (Me-MQ). Me-MQ is noted for its excellent mechanical properties, high-temperature resistance, outstanding durability, and remarkable waterproof characteristics, largely due to its long-chain spherical molecular structure. This coating also demonstrated exceptional self-cleaning capabilities, as contaminants were easily removed with water. Furthermore, it exhibited excellent durability, mechanical stability, and strong anti-ultraviolet performance [126].

2.4.4.3 Hydrophobic anti-wetting polymeric surfaces

Parts of this section have been reproduced with permission from [136]. Copyright (2022) Elsevier.

For instance, we know that lotus leaf represents remarkable anti-wetting self-cleaning properties due to the presence of hydrophobic epicuticular wax and isotropic dual (micro–nano) scale roughness papillae. Sun *et al* in their research used PDMS for its hydrophobic properties and used a nano-casting process to attain a structure similar to lotus leaf, transforming hydrophobic PDMS into a super-hydrophobic polymeric surface. The water contact angle of the PDMS before casting was 105° and after fabrication of the lotus leaf replication surface was 160° [127].

2.4.4.4 Hydrophilic anti-wetting polymeric surfaces

Parts of this section have been reproduced with permission from [136]. Copyright (2022) Elsevier.

Like hydrophobic surfaces, hydrophilic surfaces also exist naturally. Snail shell, fish scales, pitcher plants, shark skin, etc, are some common examples of such surfaces. Low drag to the surfaces and maintenance of characteristic self-cleaning properties are the result of natural hydrophilic surfaces.

Syafiq *et al* in their research prepared a smart coating using polypropylene glycol (PPG) in order to raise the surface energy of a glass substrate. Titanium dioxide was incorporated in the polymer, so as to improve surface roughness. The wettability analysis of this coating showed that the surface provided a water contact angle as low as 5° initially which suddenly reduces to 0° after 10 s of exposure. The major advantage of this type of coating is that it does not form any water streak marks over the surface of glass and provides high transparency and self-cleaning properties [128].

2.4.4.5 Flexible anti-wetting polymeric surfaces

Parts of this section have been reproduced with permission from [136]. Copyright (2022) Elsevier.

It is crucial for a coating to maintain its structural integrity and its functional properties, even upon subjection to a load or harsh environmental conditions. Polymeric materials are well known for their flexibility and adhesive properties. Polymeric materials are appropriate candidates for such coatings as their structural

integrity remains intact and protects the surfaces from harsh environmental conditions. Adding flexibility characteristics to a coating material extends its horizons of application. Usually, the flexibility of a polymeric coating is determined by the amount of binder present in the mixture and is an inverse function of this amount. Flexibility does not mean that the hardness of the coating is sacrificed, a coating material can possess both hardness and flexibility.

Choi *et al* in their research prepared a transparent flexible hard coating using organic–inorganic molecular nanocomposite siloxane linked by epoxy polymers. This particular coating provides a surface with a plastic-like modulus along with glass-like scratch resistance, as well as remarkable optical transparency [129].

2.4.5 Hydrogel and ionogel based surfaces

Once ice has been formed on a substrate, it is necessary to reduce its adhesion to the surface so that it can be removed passively, say under the influence of gravity or by drag force. In this way, the detrimental effects of ice accretion on the substrates can be avoided. The various forces of attraction between ice and the substrate are the coulomb and the van der Waals forces [130]. Ice adhesion can be reduced by weakening the atomic interactions between the surface and water molecules. This can be done by increasing the hydrophobicity of the substrate by covering the substrate by low-energy molecules. Ice adhesion can also be reduced by introduction of an insulating layer between the ice and the substrate, thereby preventing direct contact between the two. An example of this is liquid infused surfaces (LISs) and SLIPSs [66, 131]. Moving further, the ice–substrate interface always has some voids which can act as crack initiators and create stress concentration which aids in the propagation of crack at the ice–substrate interface.

In addition to this, gels also offer great potential in anti-icing applications. There is a significant amount of liquid in the gels which forms an insulating layer between the ice and the substrate and hence reduces the ice adhesion. Second, the gels reduce the apparent surface elastic modulus and cause a stiffness mismatch between the ice and the substrate. This initiates the development of interfacial cracks and helps to lower the ice adhesion [132]. The physical properties of the gels are determined by the property of liquid contained in the gel. For instance, hydrogels display hydrophilic properties as they contain plenty of water. Ionogels on the other hand exhibit high electrical conductivity as they are composed of conductive ionic liquid. In the following sections, hydrogels and ionogels are discussed in more detail.

2.4.5.1 Hydrogels

Hydrogels consist of a large quantity of water. Since water freezes at around 0 °C at normal atmospheric pressure, the common hydrogels are not able to show a high resistance to freezing at low substrate temperatures. However, by introducing suitable additives and altering the polymer networks, the hydrogels can retain their softness and other gel characteristics even at sub-zero temperatures [133]. Such modified hydrogels can also be used for anti-icing applications since they act as a lubricant between the ice and the substrate and reduce the ice adhesion. It is known

that salts help to reduce the freezing point of water and are used widely to melt the ice present on roads. Inspired by this, Li *et al* [134] developed electrolyte hydrogel (EH) surfaces by infusing salted water solution into a polyvinyl alcohol (PVA) hydrogel matrix. The resulting EH surfaces prevented ice and frost formation for an extremely long time and diminished the ice adhesion strength to an ultra-low value (Pascal level) at very low temperatures (−48.4 °C). The authors demonstrated by molecular dynamics simulations and experiments that such an extreme performance of EH surfaces is credited to the diffusion of ions to the interface between the EH and ice, as shown in the figure 2.17. The ice formed on the EH surfaces can be removed by gravity due to the ultra-low ice adhesion strength. Moreover, the salts used in the EH can be replenished by various sources such as seawater which make these EH surfaces a promising candidate in coastal infrastructure and shiphulls [134].

Inspired by antifreeze proteins, He *et al* prepared a PDMS grafted polyelectrolyte hydrogel which can be used in anti-icing applications [114]. The authors reported that by tuning the arrangement of the hydrophobic PDMS and the specificity of the ions, the properties of the interfacial water can be controlled. This controllability of the interfacial water properties provided multiple benefits. First it helped in inhibiting the ice nucleation as the ice nucleation temperature was reduced below −30 °C. Second it lowered the rate of ice propagation and finally the ice adhesion strength was also reduced (below 20 kPa).

2.4.5.2 Ionogels

Ionogels are composed of polymer networks and ionic liquids. Ionogels have been utilized widely for self-cleaning surfaces, ionic conductors and as electrolytes for batteries. Zhuo *et al* prepared an anti-icing ionogel consisting of crosslinked gelatin and 1-butyl-3-methylimidazolium bromide (BMImBr) [135]. The resultant ionogel surface inhibited ice nucleation and also controlled the ice growth rate. The authors showed that on such a surface, ice grows in an unconventional way from the water droplet–air interface towards the substrate, as shown in figure 2.18. This results in a spherical cap ice tip rather than a normal pointy cap ice. The authors further illustrated through molecular dynamics simulations as well as experiments that due to the inward ice growth and the presence of ionic liquid, an interfacial liquid layer is generated which helps to lower ice adhesion and prevent frost formation.

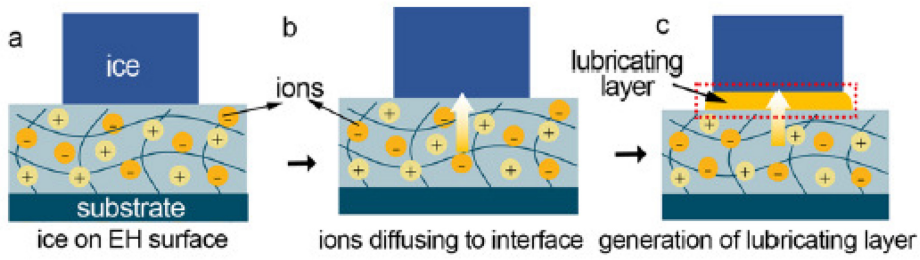

Figure 2.17. Self-generation of the lubricating layer on the EH surface. (Adapted from [134]. CC BY 4.0.)

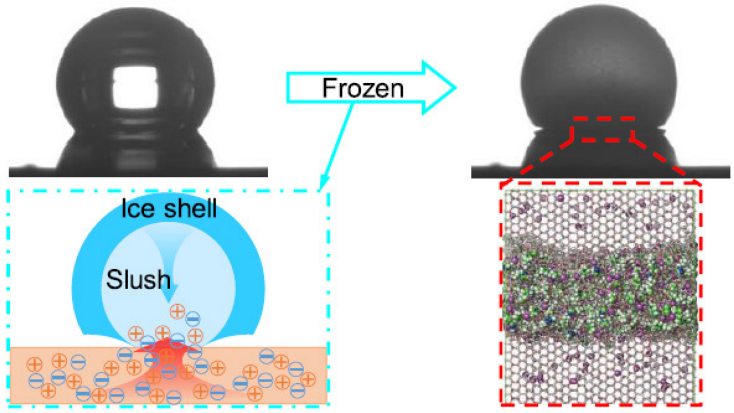

Figure 2.18. Schematic showing unconventional inward ice growth on an ionogel surface leading to a spherical ice cap and a concentrated ionic liquid aqueous interface. (Adapted with permission from [135]. Copyright (2020) American Chemical Society.)

The anti-icing potential of ionogels has been realized very recently and hence their application is currently limited. Also, some of the ionic liquids may leak into the environment and hence may be hazardous. Hence, a large effort is being made into the study of ionogels and their applications in icing considering their encouraging results in the limited studies carried out thus far.

2.5 Conclusions and perspectives

This review highlights the state-of-the-art surface chemistries relevant for anti-icing applications, detailing their advantages and limitations. Broadly, surface chemistries can be classified into fluorinated and fluorine-free categories, both of which can manifest in liquid-repellent forms that effectively reduce ice adhesion. These chemistries can be applied to surfaces in diverse forms, ranging from thin self-assembled monolayers to thicker polymers or nanocomposites.

Among the fluorinated polymers, various coatings based on materials such as polytetrafluoroethylene (PTFE) and polyvinylidene fluoride (PVDF) have been utilized. Some coatings incorporate perfluorinated end-groups ($–CF_3$), which contribute to achieving the lowest interfacial surface energy. Such coatings are recognized for their excellent chemical resistance and thermal stability. However, due to the environmental hazards associated with fluorinated compounds, there has been a significant push toward developing fluorine-free hydrophobic coatings that are more eco-friendly.

Fluorine-free polymers, particularly silicone materials such as soft polysiloxane, are commonly used in icephobic applications due to their low surface tension and energy, stemming from the inorganic Si–O bonds in their chemical structure. These silicone-based coatings can achieve ice adhesion strengths as low as 10 kPa, attributed to their softness, which induces a deformation incompatibility between the ice and the coated substrate.

Beyond polymer coatings and short-chain molecules, polyelectrolyte brushes have been prepared using surface grafting techniques. These brushes have demonstrated tunable heterogeneous ice nucleation properties by exchanging counterions, and the ice propagation rate can be adjusted by altering the hydration state of the polymer brush surfaces.

Another approach to reducing ice adhesion involves introducing a liquid layer between the ice and substrate. This liquid layer can be created using various hydrophilic, hydrophobic, or ionizable polymeric chains, with surfaces showing ice adhesion strengths below 30 kPa. SLIPSs exemplify this strategy, where a textured solid is impregnated with a lubricating liquid. SLIPSs minimize direct contact between the substrate and impacting droplets, leading to low contact angle hysteresis and allowing droplets to roll off easily, which reduces ice nucleation sites. However, SLIPSs face durability challenges, as the lubricant can be drained over time, resulting in contact line pinning of droplets.

Combining soft materials with liquid layers, gels have also emerged as potential anti-icing solutions. These gels, which can be hydrogels containing water or ionogels containing ionic liquids, provide insulation between the ice and substrate, thus reducing adhesion forces. While the application of gel-based coatings is currently limited, their promising results in preliminary studies warrant further exploration.

Recently, photo-thermal methods have been introduced for de-icing applications, utilizing Joule heating to eliminate ice on substrates. Despite its apparent simplicity, this method faces significant challenges due to high energy consumption for heat production. There is a pressing need for improved design and manufacturing of surfaces and coatings that can efficiently convert solar irradiation into heat and retain it to facilitate ice melting and removal. The integration of plasmonic effects and photo-thermal absorption with surface chemistries has shown promise in enhancing anti-icing characteristics.

Based on this review, several research opportunities for further exploration include:

- Despite tremendous progress with anti-icing features, the progress on combining durability with anti-icing characteristics needs improvement particularly when it comes to harsh applications such as those encountered in the aerospace industries and transport sectors in general.
- There is a clear need to develop halogen-free chemistries that prevent contamination of low surface tension materials, as these tend to jeopardize the anti-icing characteristics.
- There is a need to consider multi-functionality such as maintaining high or low thermal conductivity without comprising anti-icing characteristics. Molecular scale phonon-scattering and electronic transport needs to be investigated to address this.

Last, but perhaps not least, surface manufacturing techniques need to consider sustainability and scalability simultaneously in order to develop industry-ready anti-icing solutions.

References

[1] Gupta M C and Mulroney A 2020 Ice adhesion and anti-icing using microtextured surfaces *Ice Adhesion* (Beverley, MA: Scrivener) pp 389–415

[2] Grizen M and Tiwari M K 2020 Icephobic surfaces *Ice Adhesion* (Beverley, MA: Scrivener) pp 417–66

[3] Maitra T, Tiwari M K, Antonini C, Schoch P, Jung S, Eberle P and Poulikakos D 2014 On the nanoengineering of superhydrophobic and impalement resistant surface textures below the freezing temperature *Nano Lett.* **14** 172–82

[4] Maeda N 2021 Brief overview of ice nucleation *Molecules* **26** 392

[5] Li C, Liu Z, Goonetilleke E C and Huang X 2021 Temperature-dependent kinetic pathways of heterogeneous ice nucleation competing between classical and non-classical nucleation *Nat. Commun.* **12** 4954

[6] Ickes L, Welti A, Hoose C and Lohmann U 2015 Classical nucleation theory of homogeneous freezing of water: thermodynamic and kinetic parameters *Phys. Chem. Chem. Phys.* **17** 5514–37

[7] Niedermeier D, Shaw R A, Hartmann S, Wex H, Clauss T, Voigtländer J and Stratmann F 2011 Heterogeneous ice nucleation: exploring the transition from stochastic to singular freezing behavior *Atmos. Chem. Phys.* **11** 8767–75

[8] Eberle P, Tiwari M K, Maitra T and Poulikakos D 2014 Rational nanostructuring of surfaces for extraordinary icephobicity *Nanoscale* **6** 4874–81

[9] Fletcher H L 1962 *The physics of rainclouds*. By N H Fletcher. Cambridge: Cambridge University Press, 1962. pp x, 386; 99 Figures; 6 Plates. 65s *Q. J. R. Meteorolog. Soc.* **88** 559–9

[10] Golovin K, Kobaku S P R, Lee D H, DiLoreto E T, Mabry J M and Tuteja A 2016 Designing durable icephobic surfaces *Sci. Adv.* **2** e1501496

[11] Singh V, Zhang J, Chen J, Salzmann C G and Tiwari M K 2023 Precision covalent organic frameworks for surface nucleation control *Adv. Mater.* **35** 2302466

[12] Boinovich L, Emelyanenko A M, Korolev V V and Pashinin A S 2014 Effect of wettability on sessile drop freezing: when superhydrophobicity stimulates an extreme freezing delay *Langmuir* **30** 1659–68

[13] He Z, Zhuo Y, Zhang Z and He J 2021 Design of icephobic surfaces by lowering ice adhesion strength: a mini review *Coatings* **11** 1343

[14] Liu L, Wang S, Zeng X, Pi P and Wen X 2021 Dropwise condensation by nanoengineered surfaces: design, mechanism, and enhancing strategies *Adv. Mater. Interfaces* **8** 2101603

[15] Marmur A 2016 Non-wetting fundamentals *Non-wettable Surfaces: Theory, Preparation, and Applications* ed R H A Ras and A Marmur (London: The Royal Society of Chemistry)

[16] Li S, Huang J, Chen Z, Chen G and Lai Y 2017 A review on special wettability textiles: theoretical models, fabrication technologies and multifunctional applications *J. Mater. Chem.* A **5** 31–55

[17] Yong J, Chen F, Yang Q, Huo J and Hou X 2017 Superoleophobic surfaces *Chem. Soc. Rev.* **46** 4168–217

[18] Chen F, Wang Y, Tian Y, Zhang D, Song J, Crick C R, Carmalt C J, Parkin I P and Lu Y 2022 Robust and durable liquid-repellent surfaces *Chem. Soc. Rev.* **51** 8476–583

[19] He M, Wang J, Li H and Song Y 2011 Super-hydrophobic surfaces to condensed micro-droplets at temperatures below the freezing point retard ice/frost formation *Soft Matter* **7** 3993–4000

[20] Tourkine P, Le Merrer M and Quéré D 2009 Delayed freezing on water repellent materials *Langmuir* **25** 7214–6
[21] Jung S, Dorrestijn M, Raps D, Das A, Megaridis C M and Poulikakos D 2011 Are superhydrophobic surfaces best for icephobicity? *Langmuir* **27** 3059–66
[22] Lupi L and Molinero V 2014 Does hydrophilicity of carbon particles improve their ice nucleation ability? *J. Phys. Chem.* A **118** 7330–7
[23] Meuler A J, McKinley G H and Cohen R E 2010 Exploiting topographical texture to impart icephobicity *ACS Nano* **4** 7048–52
[24] Kulinich S A and Farzaneh M 2009 How wetting hysteresis influences ice adhesion strength on superhydrophobic surfaces *Langmuir* **25** 8854–6
[25] Nosonovsky M and Hejazi V 2012 Why superhydrophobic surfaces are not always icephobic *ACS Nano* **6** 8488–91
[26] Azimi Yancheshme A, Momen G and Jafari Aminabadi R 2020 Mechanisms of ice formation and propagation on superhydrophobic surfaces: a review *Adv. Colloid Interface Sci.* **279** 102155
[27] Gao L and McCarthy T J 2008 Teflon is hydrophilic. Comments on definitions of hydrophobic, shear versus tensile hydrophobicity, and wettability characterization *Langmuir* **24** 9183–8
[28] Antonini C, Villa F, Bernagozzi I, Amirfazli A and Marengo M 2013 Drop rebound after impact: the role of the receding contact angle *Langmuir* **29** 16045–50
[29] Zheng L, Li Z, Bourdo S, Khedir K R, Asar M P, Ryerson C C and Biris A S 2011 Exceptional superhydrophobicity and low velocity impact icephobicity of acetone-functionalized carbon nanotube films *Langmuir* **27** 9936–43
[30] Wang Y, Liu J, Li M, Wang Q and Chen Q 2016 The icephobicity comparison of polysiloxane modified hydrophobic and superhydrophobic surfaces under condensing environments *Appl. Surf. Sci.* **385** 472–80
[31] Kulinich S A and Farzaneh M 2009 Ice adhesion on super-hydrophobic surfaces *Appl. Surf. Sci.* **255** 8153–7
[32] Kreder M J, Alvarenga J, Kim P and Aizenberg J 2016 Design of anti-icing surfaces: smooth, textured or slippery? *Nat. Rev. Mater.* **1** 15003
[33] Antonini C, Innocenti M, Horn T, Marengo M and Amirfazli A 2011 Understanding the effect of superhydrophobic coatings on energy reduction in anti-icing systems *Cold Reg. Sci. Technol.* **67** 58–67
[34] Li W, Zhan Y and Yu S 2021 Applications of superhydrophobic coatings in anti-icing: theory, mechanisms, impact factors, challenges and perspectives *Prog. Org. Coat.* **152** 106117
[35] Huang X, Tepylo N, Pommier-Budinger V, Budinger M, Bonaccurso E, Villedieu P and Bennani L 2019 A survey of icephobic coatings and their potential use in a hybrid coating/active ice protection system for aerospace applications *Prog. Aerosp. Sci.* **105** 74–97
[36] Wu X, Zhao X, Ho J W C and Chen Z 2019 Design and durability study of environmental-friendly room-temperature processable icephobic coatings *Chem. Eng. J.* **355** 901–9
[37] 2007 *Physics and Chemistry of Ice* ed M Kuhs (London: Royal Society of Chemistry)
[38] Farhadi S, Farzaneh M and Kulinich S A 2011 Anti-icing performance of superhydrophobic surfaces *Appl. Surf. Sci.* **257** 6264–9
[39] Golovin K, Dhyani A, Thouless M D and Tuteja A 2019 Low-interfacial toughness materials for effective large-scale deicing *Science* **364** 371–5

[40] Reedy E D and Stavig M E 2020 Interfacial toughness: dependence on surface roughness and test temperature *Int. J. Fract.* **222** 1–12
[41] Chen N, Kim D H, Kovacik P, Sojoudi H, Wang M and Gleason K K 2016 Polymer thin films and surface modification by chemical vapor deposition: recent progress *Annu. Rev. Chem. Biomol. Eng.* **7** 373–93
[42] Zhuo Y, Xiao S, Amirfazli A, He J and Zhang Z 2021 Polysiloxane as icephobic materials—the past, present and the future *Chem. Eng. J.* **405** 127088
[43] He Z, Xiao S, Gao H, He J and Zhang Z 2017 Multiscale crack initiator promoted super-low ice adhesion surfaces *Soft Matter* **13** 6562–8
[44] Irajizad P, Al-Bayati A, Eslami B, Shafquat T, Nazari M, Jafari P, Kashyap V, Masoudi A, Araya D and Ghasemi H 2019 Stress-localized durable icephobic surfaces *Mater. Horiz.* **6** 758–66
[45] Wang C, Fuller T, Zhang W and Wynne K J 2014 Thickness dependence of ice removal stress for a polydimethylsiloxane nanocomposite: Sylgard 184 *Langmuir* **30** 12819–26
[46] Dou R, Chen J, Zhang Y, Wang X, Cui D, Song Y, Jiang L and Wang J 2014 Anti-icing coating with an aqueous lubricating layer *ACS Appl. Mater. Interfaces* **6** 6998–7003
[47] Koop T, Luo B, Tsias A and Peter T 2000 Water activity as the determinant for homogeneous ice nucleation in aqueous solutions *Nature* **406** 611–4
[48] Chen J, Luo Z, Fan Q, Lv J and Wang J 2014 Anti-ice coating inspired by ice skating *Small* **10** 4693–9
[49] Chen J, Dou R, Cui D, Zhang Q, Zhang Y, Xu F, Zhou X, Wang J, Song Y and Jiang L 2013 Robust prototypical anti-icing coatings with a self-lubricating liquid water layer between ice and substrate *ACS Appl. Mater. Interfaces* **5** 4026–30
[50] Heydari G, Tyrode E, Visnevskij C, Makuska R and Claesson P M 2016 Temperature-dependent deicing properties of electrostatically anchored branched brush layers of poly (ethylene oxide) *Langmuir* **32** 4194–202
[51] He Z, Xie W J, Liu Z, Liu G, Wang Z, Gao Y Q and Wang J 2016 Tuning ice nucleation with counterions on polyelectrolyte brush surfaces *Sci. Adv.* **2** e1600345
[52] Liu Z, He Z, Lv J, Jin Y, Wu S, Liu G, Zhou F and Wang J 2017 Ion-specific ice propagation behavior on polyelectrolyte brush surfaces *RSC Adv.* **7** 840–4
[53] Li C, Li X, Tao C, Ren L, Zhao Y, Bai S and Yuan X 2017 Amphiphilic antifogging/anti-icing coatings containing POSS-PDMAEMA-b-PSBMA *ACS Appl. Mater. Interfaces* **9** 22959–69
[54] Liang B, Zhang G, Zhong Z, Huang Y and Su Z 2019 Superhydrophilic anti-icing coatings based on polyzwitterion brushes *Langmuir* **35** 1294–301
[55] Landy M and Freiberger A 1967 Studies of ice adhesion: I. Adhesion of ice to plastics *J. Colloid Interface Sci.* **25** 231–44
[56] Christopher J and Wohl D H B 2019 *Contamination Mitigating Polymeric Coatings for Extreme Environments* **vol 284** (Cham: Springer Nature)
[57] Menini R and Farzaneh M 2011 Advanced icephobic coatings *J. Adhes. Sci. Technol.* **25** 971–92
[58] Mark J E 2007 *Physical Properties of Polymers Handbook* (Cham: Springer Nature)
[59] Li X, Zhao Y, Li H and Yuan X 2014 Preparation and icephobic properties of polymethyltrifluoropropylsiloxane–polyacrylate block copolymers *Appl. Surf. Sci.* **316** 222–31

[60] Murase H and Nanishi K 1985 On the relationship of thermodynamic and physical properties of polymers with ice adhesion *Ann. Glaciol.* **6** 146–9
[61] Murase H, Nanishi K, Kogure H, Fujibayashi T, Tamura K and Haruta N 1994 Interactions between heterogeneous surfaces of polymers and water *J. Appl. Polym. Sci.* **54** 2051–62
[62] Chernyy S, Järn M, Shimizu K, Swerin A, Pedersen S U, Daasbjerg K, Makkonen L, Claesson P and Iruthayaraj J 2014 Superhydrophilic polyelectrolyte brush layers with imparted anti-icing properties: effect of counter ions *ACS Appl. Mater. Interfaces* **6** 6487–96
[63] Jia Y, Yang Y, Cai X and Zhang H 2024 Recent developments in slippery liquid-infused porous surface coatings for biomedical applications *ACS Biomater. Sci. Eng.* **10** 3655–72
[64] Wang Y, Xue J, Wang Q, Chen Q and Ding J 2013 Verification of icephobic/anti-icing properties of a superhydrophobic surface *ACS Appl. Mater. Interfaces* **5** 3370–81
[65] Latthe S S, Sutar R S, Bhosale A K, Nagappan S, Ha C-S, Sadasivuni K K, Liu S and Xing R 2019 Recent developments in air-trapped superhydrophobic and liquid-infused slippery surfaces for anti-icing application *Prog. Org. Coat.* **137** 105373
[66] Wong T-S, Kang S H, Tang S K Y, Smythe E J, Hatton B D, Grinthal A and Aizenberg J 2011 Bioinspired self-repairing slippery surfaces with pressure-stable omniphobicity *Nature* **477** 443–7
[67] Bohn H F and Federle W 2004 Insect aquaplaning: nepenthes pitcher plants capture prey with the peristome, a fully wettable water-lubricated anisotropic surface *Proc. Natl Acad. Sci.* **101** 14138–43
[68] Huang C and Guo Z 2019 Fabrications and applications of slippery liquid-infused porous surfaces inspired from nature: a review *J. Bionic Eng.* **16** 769–93
[69] Li J, Ueda E, Paulssen D and Levkin P A 2019 Slippery lubricant-infused surfaces: properties and emerging applications *Adv. Funct. Mater.* **29** 1802317
[70] Heydarian S, Jafari R and Momen G 2021 Recent progress in the anti-icing performance of slippery liquid-infused surfaces *Prog. Org. Coat.* **151** 106096
[71] Sunny S, Vogel N, Howell C, Vu T L and Aizenberg J 2014 Lubricant-infused nanoparticulate coatings assembled by layer-by-layer deposition *Adv. Funct. Mater.* **24** 6658–67
[72] Zhu G H, Cho S-H, Zhang H, Zhao M and Zacharia N S 2018 Slippery liquid-infused porous surfaces (SLIPS) using layer-by-layer polyelectrolyte assembly in organic solvent *Langmuir* **34** 4722–31
[73] Juuti P *et al* 2017 Achieving a slippery, liquid-infused porous surface with anti-icing properties by direct deposition of flame synthesized aerosol nanoparticles on a thermally fragile substrate *Appl. Phys. Lett.* **110** 161603
[74] Subramanyam S B, Rykaczewski K and Varanasi K K 2013 Ice adhesion on lubricant-impregnated textured surfaces *Langmuir* **29** 13414–8
[75] Liu X, Gu H, Wang M, Du X, Gao B, Elbaz A, Sun L, Liao J, Xiao P and Gu Z 2018 3D printing of bioinspired liquid superrepellent structures *Adv. Mater.* **30** 1800103
[76] Villegas M, Cetinic Z, Shakeri A and Didar T F 2018 Fabricating smooth PDMS microfluidic channels from low-resolution 3D printed molds using an omniphobic lubricant-infused coating *Anal. Chim. Acta* **1000** 248–55
[77] Yong J, Huo J, Yang Q, Chen F, Fang Y, Wu X, Liu L, Lu X, Zhang J and Hou X 2018 Femtosecond laser direct writing of porous network microstructures for fabricating super-slippery surfaces with excellent liquid repellence and anti-cell proliferation *Adv. Mater. Interfaces* **5** 1701479

[78] Yong J, Chen F, Yang Q, Fang Y, Huo J, Zhang J and Hou X 2017 Nepenthes inspired design of self-repairing omniphobic slippery liquid infused porous surface (SLIPS) by femtosecond laser direct writing *Adv. Mater. Interfaces* **4** 1700552
[79] Liu M, Hou Y, Li J, Tie L and Guo Z 2018 Transparent slippery liquid-infused nanoparticulate coatings *Chem. Eng. J.* **337** 462–70
[80] Wang N, Xiong D, Lu Y, Pan S, Wang K, Deng Y and Shi Y 2016 Design and fabrication of the lyophobic slippery surface and its application in anti-icing *J. Phys. Chem.* C **120** 11054–9
[81] Irajizad P, Hasnain M, Farokhnia N, Sajadi S M and Ghasemi H 2016 Magnetic slippery extreme icephobic surfaces *Nat. Commun.* **7** 13395
[82] Irajizad P, Ray S, Farokhnia N, Hasnain M, Baldelli S and Ghasemi H 2017 Remote droplet manipulation on self-healing thermally activated magnetic slippery surfaces *Adv. Mater. Interfaces* **4** 1700009
[83] Liu X, Chen H, Zhao Z, Yan Y and Zhang D 2019 Slippery liquid-infused porous electric heating coating for anti-icing and de-icing applications *Surf. Coat. Technol.* **374** 889–96
[84] Singh V, Zhang J, Mandal P, Hou D, Papakonstantinou I and Tiwari M K 2024 Designing impact resistance and robustness into slippery lubricant infused porous surfaces *Adv. Mater.* **36** 2409818
[85] Cheng S, Guo P, Wang X, Che P, Han X, Jin R, Heng L and Jiang L 2022 Photothermal slippery surface showing rapid self-repairing and exceptional anti-icing/deicing property *Chem. Eng. J.* **431** 133411
[86] Laney S K, Michalska M, Li T, Ramirez F V, Portnoi M, Oh J, Thayne I G, Parkin I P, Tiwari M K and Papakonstantinou I 2021 Delayed lubricant depletion of slippery liquid infused porous surfaces using precision nanostructures *Langmuir* **37** 10071–8
[87] Villegas M, Zhang Y, Abu Jarad N, Soleymani L and Didar T F 2019 Liquid-infused surfaces: a review of theory, design, and applications *ACS Nano* **13** 8517–36
[88] Heydarian S, Maghsoudi K, Jafari R, Gauthier H and Momen G 2022 Fabrication of liquid-infused textured surfaces (LITS): the effect of surface textures on anti-icing properties and durability *Mater. Today Commun.* **32** 103935
[89] Mousavi S M, Sotoudeh F, Chun B, Lee B J, Karimi N and Faroughi S A 2024 The potential for anti-icing wing and aircraft applications of mixed-wettability surfaces—a comprehensive review *Cold Reg. Sci. Technol.* **217** 104042
[90] Liu C, Li Y, Lu C, Liu Y, Feng S and Liu Y 2020 Robust slippery liquid-infused porous network surfaces for enhanced anti-icing/deicing performance *ACS Appl. Mater. Interfaces* **12** 25471–7
[91] Shamshiri M, Jafari R and Momen G 2022 An intelligent icephobic coating based on encapsulated phase change materials (PCM) *Colloids Surf.* A **655** 130157
[92] Yuan Y, Xiang H, Liu G and Liao R 2021 Fabrication of phase change microcapsules and their applications to anti-icing coating *Surf. Interfaces* **27** 101516
[93] Irfan Lone M and Jilte R 2021 A review on phase change materials for different applications *Mater. Today Proc.* **46** 10980–6
[94] Fokaides P A, Kylili A and Kalogirou S A 2015 Phase change materials (PCMs) integrated into transparent building elements: a review *Mater. Renew. Sustain. Energy* **4** 6
[95] Kandasamy R, Wang X-Q and Mujumdar A S 2007 Application of phase change materials in thermal management of electronics *Appl. Therm. Eng.* **27** 2822–32

[96] Bentz D P and Turpin R 2007 Potential applications of phase change materials in concrete technology *Cem. Concr. Compos.* **29** 527–32
[97] Azimi Yancheshme A, Allahdini A, Maghsoudi K, Jafari R and Momen G 2020 Potential anti-icing applications of encapsulated phase change material–embedded coatings; a review *J. Energy Storage* **31** 101638
[98] Do T, Ko Y G, Chun Y and Choi U S 2015 Encapsulation of phase change material with water-absorbable shell for thermal energy storage *ACS Sustain. Chem. Eng.* **3** 2874–81
[99] Yang D, Bao R, Clare A T, Choi K-S and Hou X 2024 Phase change surfaces with porous metallic structures for long-term anti/de-icing application *J. Colloid Interface Sci.* **660** 136–46
[100] Mitridis E *et al* 2018 Metasurfaces leveraging solar energy for icephobicity *ACS Nano* **12** 7009–17
[101] Wu C *et al* 2020 Highly efficient solar anti-icing/deicing via a hierarchical structured surface *Mater. Horiz.* **7** 2097–104
[102] Dash S, de Ruiter J and Varanasi K K 2018 Photothermal trap utilizing solar illumination for ice mitigation *Sci. Adv.* **4**
[103] Wu S *et al* 2020 Superhydrophobic photothermal icephobic surfaces based on candle soot *Proc. Natl Acad. Sci.* **117** 11240–6
[104] Xie Z *et al* 2021 Carbon-based photothermal superhydrophobic materials with hierarchical structure enhances the anti-icing and photothermal deicing properties *ACS Appl. Mater. Interfaces* **13** 48308–21
[105] Xu Y *et al* 2019 Icephobic behaviors of superhydrophobic amorphous carbon nano-films synthesized from a flame process *J. Colloid Interface Sci.* **552** 613–21
[106] Wang T *et al* 2016 Passive anti-icing and active deicing films *ACS Appl. Mater. Interfaces* **8** 14169–73
[107] Volman V *et al* 2013 Radio-frequency-transparent, electrically conductive graphene nano-ribbon thin films as deicing heating layers *ACS Appl. Mater. Interfaces* **6** 298–304
[108] Zou M *et al* 2011 Effects of surface roughness and energy on ice adhesion strength *Appl. Surf. Sci.* **257** 3786–92
[109] Raji A-R *et al* 2016 Composites of graphene nanoribbon stacks and epoxy for joule heating and deicing of surfaces *ACS Appl. Mater. Interfaces* **8** 3551–6
[110] Salvati Manni L *et al* 2019 Soft biomimetic nanoconfinement promotes amorphous water over ice *Nat. Nanotechnol.* **14** 609–15
[111] Gwak Y *et al* 2015 Creating anti-icing surfaces via the direct immobilization of antifreeze proteins on aluminum *Sci. Rep.* **5** 12019
[112] Kasahara K, Waku T, Wilson P W, Tonooka T and Hagiwara Y 2020 The inhibition of icing and frosting on glass surfaces by the coating of polyethylene glycol and polypeptide mimicking antifreeze protein *Biomolecules* **10** 259
[113] Xu Y, Rong Q, Zhao T and Liu M 2020 Anti-Freezing multiphase gel materials: bioinspired design strategies and applications *Giant* **2** 100014
[114] He Z *et al* 2020 Bioinspired multifunctional anti-icing hydrogel *Matter* **2** 723–34
[115] Gao H *et al* 2017 Adaptive and freeze-tolerant heteronetwork organohydrogels with enhanced mechanical stability over a wide temperature range *Nat. Commun.* **8** 15911
[116] Koivuluoto H, Hartikainen E and Niemelä-Anttonen H 2020 Thermally sprayed coatings: novel surface engineering strategy towards icephobic solutions *Materials* **13** 1434

[117] Meuler A J *et al* 2010 Relationships between water wettability and ice adhesion *ACS Appl. Mater. Interfaces* **2** 3100–10
[118] Hejazi V, Sobolev K and Nosonovsky M 2013 From superhydrophobicity to icephobicity: forces and interaction analysis *Sci. Rep.* **3** 2194
[119] Chen J *et al* 2012 Superhydrophobic surfaces cannot reduce ice adhesion *Appl. Phys. Lett.* **101** 111603
[120] Jung S *et al* 2011 Are superhydrophobic surfaces best for icephobicity? *Langmuir* **27** 3059–66
[121] Kulinich S A, Farhadi S, Nose K and Du X W 2011 Superhydrophobic surfaces: are they really ice-repellent? *Langmuir* **27** 25–9
[122] Wu X, Silberschmidt V v, Hu Z-T and Chen Z 2019 When superhydrophobic coatings are icephobic: role of surface topology *Surf. Coat. Technol.* **358** 207–14
[123] Tagliaro I, Cerpelloni A, Nikiforidis V-M, Pillai R and Antonini C 2022 On the development of icephobic surfaces: bridging experiments and simulations *The Surface Wettability Effect on Phase Change* (Cham: Springer International) pp 235–72
[124] Xie H *et al* 2021 Waterborne, non-fluorinated and durable anti-icing superhydrophobic coatings based on diatomaceous earth *New J. Chem.* **45** 10409–17
[125] Xie H *et al* 2022 Non-fluorinated and durable photothermal superhydrophobic coatings based on attapulgite nanorods for efficient anti-icing and deicing *Chem. Eng. J.* **428** 132585
[126] Wu Y *et al* 2022 Nonfluorinated, transparent, and antireflective hydrophobic coating with self-cleaning function *Colloids Surf.* A **634** 127919
[127] Sun M *et al* 2005 Artificial lotus leaf by nanocasting *Langmuir* **21** 8978–81
[128] Syafiq A, Vengadaesvaran B, Pandey A K and Abd Rahim N 2018 Superhydrophilic smart coating for self-cleaning application on glass substrate *J. Nanomater.* **2018**
[129] Choi G M *et al* 2017 Flexible hard coating: glass-like wear resistant, yet plastic-like compliant, transparent protective coating for foldable displays *Adv. Mater.* **29** 1700205
[130] Xiao S, Skallerud B H, Wang F, Zhang Z and He J 2019 Enabling sequential rupture for lowering atomistic ice adhesion *Nanoscale* **11** 16262–9
[131] Kim P *et al* 2012 Liquid-infused nanostructured surfaces with extreme anti-ice and anti-frost performance *ACS Nano* **6** 6569–77
[132] Kevin G *et al* 2021 Designing durable icephobic surfaces *Sci. Adv.* **2** e1501496–e16
[133] Jian Y *et al* 2021 Biomimetic anti-freezing polymeric hydrogels: keeping soft-wet materials active in cold environments *Mater. Horiz.* **8** 351–69
[134] Li T *et al* 2020 Self-deicing electrolyte hydrogel surfaces with Pa-level ice adhesion and durable antifreezing/antifrost performance *ACS Appl. Mater. Interfaces* **12** 35572–8
[135] Zhuo Y, Xiao S, Håkonsen V, He J and Zhang Z 2020 Anti-icing ionogel surfaces: inhibiting ice nucleation, growth, and adhesion *ACS Mater. Lett.* **2** 616–23
[136] Paras and Kumar A 2022 Anti-wetting polymeric coatings *Encyclopedia of Materials: Plastics and Polymers* vol 2 (Amsterdam: Elsevier) pp 786–95